Advances in Computational Design, *Vol. 5, No. 1 (2020) 55-89*
DOI: https://doi.org/10.12989/acd.2020.5.1.055

Analytical free vibration solution for angle-ply piezolaminated plate under cylindrical bending: A piezo-elasticity approach

Agyapal Singh[a] and Poonam Kumari*

Department of Mechanical Engineering, Indian Institute of Technology Guwahati, Guwahati 781039, India

(Received May 21, 2019, Revised August 13, 2019, Accepted August 28, 2019)

Abstract. For the first time, an accurate analytical solution, based on coupled three-dimensional (3D) piezoelasticity equations, is presented for free vibration analysis of the angle-ply elastic and piezoelectric flat laminated panels under arbitrary boundary conditions. The present analytical solution is applicable to composite, sandwich and hybrid panels having arbitrary angle-ply lay-up, material properties, and boundary conditions. The modified Hamiltons principle approach has been applied to derive the weak form of governing equations where stresses, displacements, electric potential, and electric displacement field variables are considered as primary variables. Thereafter, multi-term multi-field extended Kantorovich approach (MMEKM) is employed to transform the governing equation into two sets of algebraic-ordinary differential equations (ODEs), one along in-plane (x) and other along the thickness (z) direction, respectively. These ODEs are solved in closed-form manner, which ensures the same order of accuracy for all the variables (stresses, displacements, and electric variables) by satisfying the boundary and continuity equations in exact manners. A robust algorithm is developed for extracting the natural frequencies and mode shapes. The numerical results are reported for various configurations such as elastic panels, sandwich panels and piezoelectric panels under different sets of boundary conditions. The effect of ply-angle and thickness to span ratio (s) on the dynamic behavior of the panels are also investigated. The presented 3D analytical solution will be helpful in the assessment of various 1D theories and numerical methods.

Keywords: free vibration; extended Kantorovich method (EKM); analytical solution; angle-ply piezoelectric laminate; arbitrary boundary conditions; smart structures

1. Introduction

Nowadays, composite and sandwich structures are replacing the metal parts in every field of engineering i.e., aerospace, marine, automobile, etc. because of their attractive properties such as high specific strength, lightweight, damage tolerance, energy absorption capabilities and buckling resistance, etc. In this direction, a decade ago, the researchers introduced the concept of smart structures in which active material (piezoelectric) layers are integrated with host laminates. These structures are known as smart/adaptive or intelligent structures which can be used for health monitoring and vibration control purpose. Such hybrid (smart) structures are subjected to various loadings (static and dynamic loads) and boundary conditions. Due to electromechanical coupling

*Corresponding author, Associate Professor, E-mail: kpmech@iitg.ac.in
[a] Ph.D. Student, E-mail: agyapal@iitg.ac.in

http://www.techno-press.org/?journal=acd&subpage=7 ISSN: 2383-8477 (Print), 2466-0523 (Online)

in such piezoelectric laminates, the behavior of structure (like edge effect) is more complex and can lead to peeling of the piezoelectric actuator's and sensor's layers. Understanding their bending, buckling and free vibration behavior, with sufficient accuracy has gained research interest. Thus many mathematical models have been developed to predict the behavior of composite plates, sandwich plates, and piezoelectric laminated structures. Knowledge of fundamental frequencies and mode shapes are very much required for efficient design of smart structures. Three-dimensional (3D) semi-analytical/analytical solutions can accurately predict the natural frequencies and influence of electromechanical coupling.

Five decades ago, Jones (1970) presented an exact free vibration solution for cross-ply simply supported plate under plane strain condition (cylindrical bending). Further, Jones (1971) extended this approach to free vibration solution of angle-ply panels. After a long gap, Heyliger and Brooks (1995) further extended this elastic solution to piezoelectric case where an exact solution was developed to acquire natural frequencies and through-thickness modal distributions of the simply-supported cross-ply piezoelectric plate in cylindrical bending. Further, Kumari *et al.* (2007) presented 2D exact solutions for harmonic analysis of flat hybrid piezoelectric and magnetoelastic angle-ply panels under the simply-supported boundary conditions. By employing the Fourier series method, Yang *et al.* (1994) obtained the forced vibration response of composite elastic panels mounted with piezoelectric actuator layers at the top and bottom surfaces. By employing Stroh formalism, Vel *et al.* (2004) presented an analytical technique to study the free vibrations of laminated elastic panels with either embedded or surface mounted piezoelectric patches of arbitrary thickness and width. Chen and Lee (2004) presented the 3D free vibration solution of arbitrary supported cross-ply laminate in cylindrical bending using semi-analytical approach SSDQM (state space approach along the thickness and differential quadrature method (DQM) along in-plane direction). Using SSDQM, Zhou *et al.* (2009) develop a semi-analytical free vibration solution for arbitrary supported orthotropic piezoelectric cross-ply flat panels. Further, Zhou *et al.* (2010) extended this approach to investigate the static and dynamic behaviour of cross-ply piezoelectric panels with interlaminar bonding imperfections. Very recently, Udayakumar and Gopal (2017) employed a modified state-space differential quadrature method to develop a dynamic solution for thick sandwich panels having softcore with general edge support conditions. Ebrahimi and Barati (2016) investigated the thermal stability of magneto-electro-thermo-elastic functionally graded (METE-FG) nanoplates based on the nonlocal theory and a refined plate model. Ebrahimi and Barati (2017a) developed a nonlocal strain gradient plate model for vibration analysis of smart piezoelectric polymeric nanoplates resting on viscoelastic medium with damping. Ebrahimi and Barati (2017b) presented an analytical model to studies the effects of the magnetic field on the free vibration behavior of magneto-electro-elastic functionally graded smart nanoplates (MEE-FG) under different support conditions. By using the refined four-variable plate theory, Barati and Zenkour (2018) developed an analytical solution for electro-thermo-mechanical vibrational analysis of functionally graded piezoelectric (FGP) plates with porosities. Very recently, Abad and Rouzegar (2019) presented exact wave propagation analysis for moderately thick Levy-type plate integrated with piezoelectric layers using the spectral element method. The present literature survey is limited to the free vibration analysis of panels. The detailed literature about the mathematical models and solution techniques to analyze the static and the dynamic behavior of laminates can found in review articles (Sayyad and Ghugal, 2015; Wu and Liu, 2016). Very recently, Yan *et al.* (2019) presented a 3D exact solution for the analysis of imperfect angle-ply smart plate in cylindrical bending and subjected to simply-supported boundary condition. KelvinVoigt viscoelastic model is implemented to describe the interfacial properties and state-

space method is applied to obtain the solution of simply-supported angle-ply panels with surface-bonded piezoelectric layers.

As 3D solutions of piezoelectric laminates involve complex mathematics and further extracting the natural frequencies is even more challenging. Therefore, two-dimensional solutions also have been proposed in this area. Using classical plate theory (CLT) and first-order shear deformation theory (FSDT), Khdeir (2001) obtained the free and forced vibration solution of the anti-symmetric angle-ply flat panels under general boundary conditions. Messina (2001) investigated the free vibration behavior of angle-ply composite multilayered panels using higher-order plate theories. Further, Messina and Soldatos (2002) extended it to the dynamic case, where 2D parabolic shear deformable plate theory was used. This theory satisfies the inter-laminar continuity of both shear stresses and displacements for the arbitrary stacking pattern. Based on equivalent single layer approximation, Shu (2005a) developed an accurate theory to obtain the free vibration response of cross-ply piezoelectric laminates subjected to an arbitrary combination of boundary conditions. Further, Shu (2005b) extended this approach to study static and free vibration behaviors of the cross-ply piezoelectric plate under cylindrical bending with interfacial shear slip. Kim (2007) developed two enhanced theories namely EFSDT (enhanced first-order shear deformation theory) and EHSDT (enhanced higher-order shear deformation theory) for composite and sandwich plates based on the mixed variational formulation and obtained analytical free vibration solutions for angle-ply simply-supported plates in cylindrical bending. Recently, Behera and Kumari (2018) presented an exact analytical free vibration solution for Levy-type rectangular laminated plate based on efficient Zig-Zag theory (ZIGT) and third-order theory (TOT). However, two-dimensional solutions cannot provide accurate free vibration response for thick laminates (Sayyad and Ghugal 2015).

Three-dimensional (3D) solutions can provide more accurate insight into local and global behavior of vibrating plates as compared to 2D methods. Further, 3D solutions serve as the benchmark for assessing the two-dimensional theories and other numerical methods for analyzing composite and piezoelectric plates accurately. In literature researchers used different approaches, namely Pagano's classical approach by Heyliger and Brooks (1995); Heyliger and Saravanos (1995); Heyliger and Brooks (1996); Pan and Heyliger (2003), the state space approach by Yang *et al.* (1994, 1995) ; Batra and Liang (1997); Xu *et al.* (1997); Chen and Ding (2002); Sheng *et al.* (2007), the series expansion approach by Dube *et al.* (1996a,b); Hussein and Heyliger (1998) and the asymptotic approach by Cheng *et al.* (1999, 2000); Cheng and Batra (2000a,b), extended Kantorovich method by Kapuria and Kumari (2012); Kumari and Behera (2017a); Behera and Kumari (2019); Kapuria and Dhanesh (2017), to develop analytical 3D solution for plate structures. The limitation of exact and analytical solution is that these solutions are limited only to a certain type of boundary condition, geometry, and configurations due to the mathematical complexity of the problems. Besides from this, some authors develop semi-analytical approaches, like state-space conjunction with differential quadrature method (SSDQM) by Chen and Lee (2004); Zhou *et al.* (2009); Chen and Lü (2005) to get 3D elasticity solutions for laminated composite and piezoelectric plates. However, DQM has also a limitation of handling complex boundary conditions and irregular geometries pertaining to is the global approach. Therefore, some pure numerical approaches, like 3D finite element (Balabaev and Ivina, 2014), 3D differential quadrature(Zhang *et al.* 2006) and 3D meshless methods (Zhang *et al.* 2006), are also used to develop a 3D elastic based solution for plate structures. However, the limitation of numerical techniques is that it cannot provide continuous transverse stresses through-thickness and predict artificial high natural frequencies (Qing *et al.* 2006). For a detailed review on 3D mathematical

modeling for laminated composite and piezoelectric structures, one can refer some review article given by Saravanos and Heyliger (1999); Wu *et al.* (2008); Kapuria *et al.* (2010); Wu and Liu (2016); Singhatanadgid and Singhanart (2019); Sayyad and Ghugal (2015).

Based on the literature survey, it is observed that no three-dimensional analytical solution exists for free vibration analysis of angle-ply laminated piezoelectric panel under arbitrary boundary conditions. Zhou *et al.* (2009) also stated that usually for such cases the coupled piezo-elasticity analytical solutions are very difficult to drive. Hence, an efficient analytical solution method is needful to predict the complex dynamic behavior of arbitrarily supported piezoelectric laminated panels, which will also act as a benchmark for assessing other approximate or numerical method. Analytical techniques are preferred because of their simplicity and high accuracy. Moreover, the closed-form 3D piezo-elasticity solution helps to understand the complex electromechanical behavior of hybrid panels and helps to make a suitable assumption for the kinematic and the kinetic field for 1D/2D plate theories.

The detailed literature on extended Kantorovich method (EKM) can be found in a recent review paper presented by Singhatanadgid and Singhanart (2017). Kapuria and Kumari group developed an extended Kantorovich approach to analyze the various problem of elastic, piezoelectric and functionally graded plates (Kapuria and Kumari, 2011, 2012, 2013; Kumari *et al.* 2014; Kumari and Behera, 2017b; Behera and Kumari, 2019; Kumari *et al.* 2017; Singh *et al.* 2018). Recently using EKM, Kumari and Behera (2017b) developed three-dimensional elasticity solution for free vibration analysis of elastic laminated plates subjected to Levy-type supports. Further, Behera and Kumari (2019) extended this approach to develop 3D free vibration solution for a piezoelectric composite plate under Levy-type support conditions. But above proposed solutions (Kumari and Behera, 2017b; Behera and Kumari, 2019) are only applicable to cross-ply rectangular plates subjected to Levy-type boundary conditions. Many engineering structures, such as turbine blades, tank bottom, floors and roof of the building, often modeled as flat panels which are subjected to arbitrary boundary conditions. In this paper, the above multi-term EKM approach is extended to develop a 3D free vibration solution for angle-ply elastic and piezoelectric panels subjected to arbitrary boundary conditions.

The aim of the present paper is to develop an accurate analytical solution based on coupled threedimensional (3D) piezo-elasticity equations for free vibration analysis of the angle-ply elastic and piezoelectric flat laminated plates in cylindrical bending. The significant novelties and contributions of present work are given below

- For the first time, a fully coupled three-dimensional (3D) piezo-elasticity analysis is presented for angle-ply piezoelectric flat laminated panels.
- Side edges can have any combination of mechanical boundary condition. For example, Simple supported(S–S), Clamped-Clamped (C–C), Clamped-Free (C–F), Clamped-Simply supported (C–S)
- Side edges and top/bottom surfaces of the panel can have different electric boundary conditions i.e., open or closed circuit boundary conditions.
- Interface continuity and boundary condition are satisfied in exact manners which ensures the same order of accuracy for all the variables (stresses, displacements, and electric variables)
- The present solution is valid for thick as well as thin flat laminated composite and piezoelectric panels.
- First five fundamental frequencies are tabulated for various configuration and lay-ups. Free vibration behavior of highly inhomogeneous composite panels is also investigated. (To the best of the author's knowledge not available in the literature)

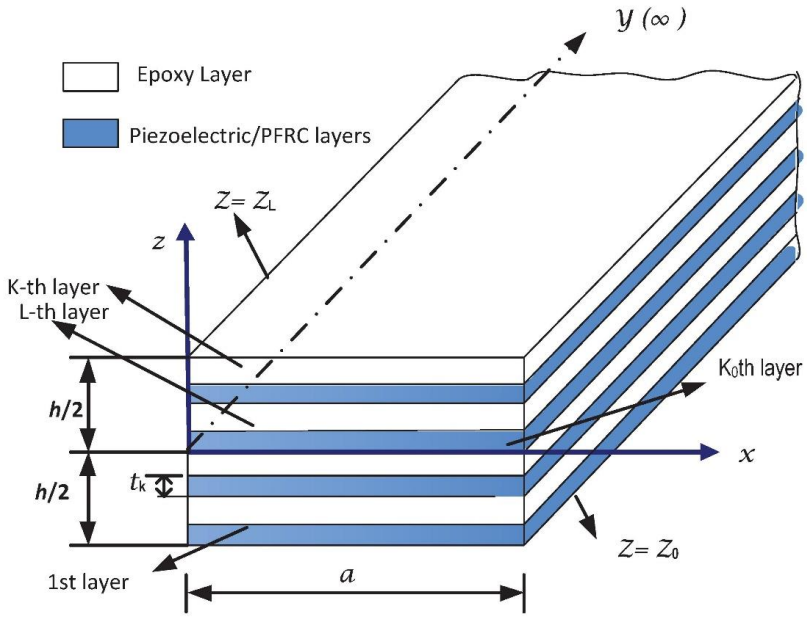

Fig. 1 Geometry of the Piezoelectric-laminated panel.

- The presented 3D analytical solution is able to predict the effect of electric boundary condition on the natural frequencies of piezoelectric laminated panels. Thought the effect is not very significant due to the weak coupling between the electric and elastic fields. However, these small effects are very much important to detect accurately for precise control applications.
- Longitudinal variation of displacement and stresses for various cases are also presented for different support conditions.

2. Governing equations of angle-ply piezoelectric-laminated panels

An infinitely long (along y-direction) angle-ply piezoelectric laminated panel of total thickness h along the z-axis and having length a along direction of x-axis, as shown in Fig. 1, is considered for modeling (cylindrical bending case). The hybrid laminated panel has L number of perfectly bonded laminas which is generally orthotropic and a few of them can be orthotropic piezoelectric/PFRC material which could be utilized as distributed sensors and actuators, and these piezoelectric/PFRC laminas are poled along the thickness z-direction. The governing equations hold for each k^{th} layer having thickness $t(k)$, and its bottommost face is denoted by z_{k-1}. Where the interface of k^{th} and k+1th ply symbolized as the k^{th} interface. Generally, the plane strain condition is $\varepsilon_y = \gamma_{xy} = \gamma_{yz} = 0$. These conditions are applicable for the cross-ply plate under cylindrical bending. But these assumptions are not applicable to the angle-ply case. So, generalized plane strain conditions are used to predict the behavior of the angle-ply laminated plate accurately. In generalized plane strain, the displacements of the plate are independent of y-coordinate and it is the only function of x- and z- coordinate. Therefore, $\varepsilon_y = 0$, $\gamma_{xy} \neq 0$, $\gamma_{yz} \neq 0$ (Kapuria and Kumari 2013). Based on these conditions, strain-displacement and electric field-potential correlations reduce to,

$$\begin{bmatrix}\varepsilon_x\\ \varepsilon_y\\ \varepsilon_z\end{bmatrix}=\begin{bmatrix}u_{,x}\\ 0\\ w_{,z}\end{bmatrix},\qquad \begin{bmatrix}\gamma_{xy}\\ \gamma_{zx}\\ \gamma_{yz}\end{bmatrix}=\begin{bmatrix}v_{,x}\\ w_{,x}+u_{,z}\\ v_{,z}\end{bmatrix},\qquad \begin{bmatrix}E_x\\ E_y\\ E_z\end{bmatrix}=\begin{bmatrix}-\phi_{,x}\\ 0\\ -\phi_{,z}\end{bmatrix} \tag{1}$$

where u, v and w are displacements and E_x, E_y, E_z are electric field components along x, y and z-direction, respectively, which are independent of y and only functions of x and z coordinates. ϕ denotes electric potential and a subscript comma represents partial differentiation. The coupled 3D piezo-elasticity constitutive equations for the angle-ply case are given as (Kapuria and Kumari 2013),

$$\begin{aligned}
\varepsilon_x &= \bar{s}_{11}\sigma_x + \bar{s}_{12}\sigma_y + \bar{s}_{13}\sigma_z + \bar{s}_{16}\tau_{xy} + \bar{d}_{31}E_z\\
\varepsilon_y &= \bar{s}_{12}\sigma_x + \bar{s}_{22}\sigma_y + \bar{s}_{23}\sigma_z + \bar{s}_{26}\tau_{xy} + \bar{d}_{32}E_z\\
\varepsilon_z &= \bar{s}_{13}\sigma_x + \bar{s}_{23}\sigma_y + \bar{s}_{33}\sigma_z + \bar{s}_{36}\tau_{xy} + \bar{d}_{33}E_z\\
\gamma_{yz} &= \bar{s}_{44}\tau_{yz} + \bar{s}_{45}\tau_{zx} + \bar{d}_{14}E_x + \bar{d}_{24}E_y\\
\gamma_{zx} &= \bar{s}_{54}\tau_{yz} + \bar{s}_{55}\tau_{zx} + \bar{d}_{15}E_x + \bar{d}_{25}E_y\\
\gamma_{xy} &= \bar{s}_{16}\sigma_x + \bar{s}_{26}\sigma_y + \bar{s}_{36}\sigma_z + \bar{s}_{66}\tau_{xy} + \bar{d}_{36}E_z\\
D_x &= \bar{d}_{14}\tau_{yz} + \bar{d}_{15}\tau_{zx} + \bar{\epsilon}_{11}E_x + \bar{\epsilon}_{12}E_y\\
D_y &= \bar{d}_{24}\tau_{yz} + \bar{d}_{25}\tau_{zx} + \bar{\epsilon}_{21}E_x + \bar{\epsilon}_{22}E_y\\
D_z &= \bar{d}_{31}\sigma_x + \bar{d}_{32}\sigma_y + \bar{d}_{33}\sigma_z + \bar{d}_{36}\tau_{xy} + \bar{\epsilon}_{33}E_z
\end{aligned} \tag{2}$$

where σ_i and ε_i denotes the normal stress and normal strains components, respectively. τ_{ij} and γ_{ij} denotes shear stress and shear strains, respectively. D_i denotes the electric displacements and $\bar{s}_{ij}$ represent the transformed elastic compliances. Where $\bar{\epsilon}_{ij}$ and $\bar{d}_{ij}$ represent dielectric permittivity constants and piezoelectric strain constants at constant stress field, respectively. Using Eq. $(2)_9$, E_z can be represented in terms of D_z as

$$E_z = -\bar{d}'_{31}\sigma_x - \bar{d}'_{32}\sigma_y - \bar{d}'_{33}\sigma_z - \bar{d}'_{36}\tau_{xy} + \frac{1}{\bar{\epsilon}_{33}}D_z \tag{3}$$

where $\bar{d}'_{ij} = \bar{d}_{ij}/\bar{\epsilon}_{33}$. Evaluate ε_y from Eq. $(1)_2$ and E_z from Eq. (3) and substituting in Eq. $(2)_2$, σ_y is written as

$$\sigma_y = -(\bar{d}'_{32}/\bar{s}'_{22})D_z - (\bar{s}'_{23}/\bar{s}'_{22})\sigma_z - (\bar{s}'_{26}/\bar{s}'_{22})\tau_{xy} - (\bar{s}'_{12}/\bar{s}'_{22})\sigma_x \tag{4}$$

where $\bar{s}'_{ij} = \bar{s}_{ij} - \bar{d}_{3j}\bar{d}_{3i}/\bar{\epsilon}_{33}$. Using Eqs. (3) and (4), E_z and σ_y can be eliminated from Eqs. $(2)_1$, $(2)_3$, $(2)_6$ and Eq. (3) which yield

$$\begin{aligned}
\varepsilon_x &= p_{11}\sigma_x + p_{16}\tau_{xy} + p_{13}\sigma_z + p_{18}D_z\\
\varepsilon_z &= p_{31}\sigma_x + p_{36}\tau_{xy} + p_{33}\sigma_z + p_{38}D_z\\
\gamma_{xy} &= p_{61}\sigma_x + p_{66}\tau_{xy} + p_{63}\sigma_z + p_{68}D_z\\
E_z &= -(p_{81}\sigma_x + p_{86}\tau_{xy} + p_{83}\sigma_z + p_{88}D_z)
\end{aligned} \tag{5}$$

Where

$$\begin{aligned} p_{ij} &= \bar{s}'_{ij} - \bar{s}'_{2j}\bar{s}'_{2i}/\bar{s}'_{22}, & p_{88} &= -1/\bar{\epsilon}_{33} - \bar{d}'^{2}_{32}/\bar{s}'_{22} \\ p_{i8} &= p_{8i} = \bar{d}'_{3i} - \bar{d}'_{32}\bar{s}'_{2i}/\bar{s}'_{22} & &\text{for } (i,j) = 1,3 \text{ and } 6 \end{aligned} \tag{6}$$

Again, substituting the Eq. $(2)_2$ in Eq. $(1)_2$, σ_y can be written as

$$\sigma_y = -(\bar{d}_{32}/\bar{s}_{22})E_z - (\bar{s}_{23}/\bar{s}_{22})\sigma_z - (\bar{s}_{26}/\bar{s}_{22})\tau_{xy} - (\bar{s}_{12}/\bar{s}_{22})\sigma_x \tag{7}$$

Again, using σ_y from Eq. (7) into Eqs. $(2)_1$, $(2)_3$, $(2)_6$ and $(2)_9$, ε_x, ε_z, γ_{xy} and E_z can be written in terms of σ_x, τ_{xy}, σ_z and E_z as

$$\begin{aligned} \varepsilon_x &= \bar{p}_{11}\sigma_x + \bar{p}_{16}\tau_{xy} + \bar{p}_{13}\sigma_z + \bar{p}_{18}E_z \\ \varepsilon_z &= \bar{p}_{31}\sigma_x + \bar{p}_{36}\tau_{xy} + \bar{p}_{33}\sigma_z + \bar{p}_{38}E_z \\ \gamma_{xy} &= \bar{p}_{61}\sigma_x + \bar{p}_{66}\tau_{xy} + \bar{p}_{63}\sigma_z + \bar{p}_{68}E_z \\ E_z &= -(\bar{p}_{81}\sigma_x + \bar{p}_{86}\tau_{xy} + \bar{p}_{83}\sigma_z + \bar{p}_{88}D_z) \end{aligned} \tag{8}$$

where

$$\begin{aligned} &\bar{p}_{ij} = \bar{s}_{ij} - \bar{s}_{2j}\bar{s}_{2i}/\bar{s}_{22}, \quad \bar{p}_{88} = -1/[\bar{\epsilon}_{33} - (\bar{d}_{32})^2/\bar{s}_{22}], \quad \bar{p}_{i8} = \bar{d}_{3i} - \bar{s}_{2i}\bar{d}_{32}/\bar{s}_{22} \\ &\bar{p}_{8i} = (\bar{d}_{3i} - \bar{s}_{2i}\bar{d}_{32}/\bar{s}_{22})/[\bar{\epsilon}_{33} - (\bar{d}_{32})^2/\bar{s}_{22}], \quad \text{for} \quad (i,j) = 1,3 \text{ and } 6 \end{aligned} \tag{9}$$

Utilizing Eqs. $(2)_4$, $(2)_5$ and $(2)_7$, γ_{yz}, γ_{zx} and E_x can also be written in terms of τ_{yz}, τ_{zx} and D_x as

$$\gamma_{yz} = p_{44}\tau_{yz} + p_{45}\tau_{zx} + p_{47}D_x \tag{10}$$

$$\gamma_{zx} = p_{54}\tau_{yz} + p_{55}\tau_{zx} + p_{57}D_x \tag{11}$$

$$E_x = -p_{74}\tau_{yz} - p_{75}\tau_{zx} + p_{77}D_x \tag{12}$$

where

$$\begin{aligned} &p_{ij} = \bar{s}_{ij} - \bar{d}_{1i}\bar{d}_{1j}/\bar{\epsilon}_{11}, \quad p_{47} = \bar{d}_{14}/\bar{\epsilon}_{11}, \quad p_{74} = p_{47}, \\ &p_{77} = 1/\bar{\epsilon}_{11}, \quad p_{57} = p_{75} = \bar{d}_{15}/\bar{\epsilon}_{11} \qquad \text{for}(i,j) = (4,5) \end{aligned} \tag{13}$$

Piezo-elasticity based extended Hamilton principle in a mixed form, without any internal charge and body force source, for the cylindrical bending case can be expressed as, (Behera and Kumari 2019):

$$\begin{aligned} &\int_t \int_a \int_h [\delta u(\sigma_{x,x} + \tau_{xz,z} - \rho\ddot{u}) + \delta v(\tau_{xy,x} + \tau_{yz,z} - \rho\ddot{v}) + \delta w(\tau_{zx,x} + \sigma_{z,z} - \rho\ddot{w}) + \delta\phi(D_{x,x} + D_{z,z}) \\ &+ \delta\sigma_x(\varepsilon_x - u_{,x}) + \delta\sigma_z(\varepsilon_z - w_{,z}) + \delta\tau_{yz}(\gamma_{yz} - v_{,z}) + \delta\tau_{zx}(\gamma_{zx} - u_{,z} - w_{,x}) + \delta\tau_{xy}(\gamma_{xy} - v_{,x}) \\ &- \delta D_x(E_x + \phi_{,x}) - \delta D_z(E_z + \phi_{,z})]\, dz\ dx\ dt = 0 \end{aligned} \tag{14}$$

From Eqs. (5) and (10)-(12), the expressions of strain and electric field components (ε_x, ε_z, γ_{xy}, γ_{yz}, γz_x, E_z and E_x) substituting into Eq. (14) yields

$$\int_t\int_a\int_h [\delta u(\tau_{xz,z}+\sigma_{x,x}-\rho\ddot{u})+\delta v(\tau_{yz,z}+\tau_{xy,x}-\rho\ddot{v})+\delta w(\sigma_{z,z}+\tau_{zx,x}-\rho\ddot{w})+\delta\phi(D_{x,x}+D_{z,z})$$
$$+\delta\sigma_x(p_{11}\sigma_x+p_{16}\tau_{xy}+p_{13}\sigma_z+p_{18}D_z-u_{,x})+\delta\sigma_z(p_{31}\sigma_x+p_{36}\tau_{xy}+p_{33}\sigma_z+p_{38}D_z-w_{,z})$$
$$+\delta\tau_{yz}(p_{44}\tau_{yz}+p_{45}\tau_{zx}+p_{47}D_x-v_{,z})+\delta\tau_{zx}(p_{54}\tau_{yz}+p_{55}\tau_{zx}+p_{57}D_x-u_{,z}-w_{,x}) \quad (15)$$
$$+\delta\tau_{xy}(p_{61}\sigma_x+p_{66}\tau_{xy}+p_{63}\sigma_z+p_{68}D_z-v_{,x})+\delta D_x(p_{74}\tau_{yz}+p_{75}\tau_{zx}-p_{77}D_x-\phi_{,x})$$
$$-\delta D_z(\phi_{,z}-p_{81}\sigma_x-p_{86}\tau_{xy}-p_{83}\sigma_z-p_{88}D_z)]\,dz\,dx\,dt=0$$

This form of the variational equation is used when the solution in x direction is considered as known and the ODEs are formed for the z direction. When the solution is known in z direction, and the ODEs are to be formed for the x direction, the alternative expressions for ε_x, ε_z, γ_{xy} and E_z from Eq. (8) are substituted in Eq. (14) to yield

$$\int_t\int_a\int_h [\delta u(\tau_{xz,z}+\sigma_{x,x}-\rho\ddot{u})+\delta v(\tau_{yz,z}+\tau_{xy,x}-\rho\ddot{v})+\delta w(\sigma_{z,z}+\tau_{zx,x}-\rho\ddot{w})+\delta\phi(D_{x,x}+D_{z,z})$$
$$+\delta\sigma_x(\bar{p}_{11}\sigma_x+\bar{p}_{16}\tau_{xy}+\bar{p}_{13}\sigma_z+\bar{p}_{18}E_z-u_{,x})+\delta\sigma_z(\bar{p}_{31}\sigma_x+\bar{p}_{36}\tau_{xy}+\bar{p}_{33}\sigma_z+\bar{p}_{38}E_z-w_{,z})$$
$$+\delta\tau_{yz}(p_{44}\tau_{yz}+p_{45}\tau_{zx}+p_{47}D_x-v_{,z})+\delta\tau_{zx}(p_{54}\tau_{yz}+p_{55}\tau_{zx}+p_{57}D_x-u_{,z}-w_{,x}) \quad (16)$$
$$+\delta\tau_{xy}(\bar{p}_{61}\sigma_x+\bar{p}_{66}\tau_{xy}+\bar{p}_{63}\sigma_z+\bar{p}_{68}E_z-v_{,x})+D_x(p_{74}\tau_{yz}+p_{75}\tau_{zx}-p_{77}D_x-\phi_{,x})$$
$$-\delta D_z(\phi_{,z}-\bar{p}_{81}\sigma_x-\bar{p}_{86}\tau_{xy}-\bar{p}_{83}\sigma_z-\bar{p}_{88}D_z)]\,dz\,dx\,dt=0$$

It may be noted that Eqs. (15) and (16) are identical for the elastic case. Here, t is the time variable. Where dimensionless in-plane coordinates $\xi=x/a$ along the x-direction and thickness coordinate $\zeta=(z-z_{k-1})/t^{(k)}$ for a layer along the z-direction are defined which varies from 0 to 1. The support conditions considered at the top and bottom surface are: at $z=\pm h/2$: $\sigma_z=0,\quad \tau_{yz}=0,\quad \tau_{zx}=0,\quad \phi=0$ or $D_z=0$. For perfect bounding, the equilibrium continuity conditions at the interface between k^{th} and k+1th laminas are given as, (Kapuria and Kumari 2013)

$$[(u, v, w, \sigma_z, \tau_{yz}, \tau_{zx}, \phi, D_z)|_{\zeta=1}]^{(k)}=[(u, v, w, \sigma_z, \tau_{yz}, \tau_{zx}, \phi, D_z)|_{\zeta=0}]^{(k+1)} \quad (17)$$

The interfaces of piezoelectric layers with the elastic layers are always assumed as grounded ($\phi=0$) for effective sensing/actuation. Along x-axis, panel can have any type of mechanical support such as, Simply supported (S): σ_x = 0, w=0, τ_{xy} =0; Free (F): τ_{xz} =0, σ_x = 0, τ_{xy} =0 ; Clamped (C): u=0, w=0, v=0. The ends (x=0, a) can have the closed-circuit condition (CC) in which potential is prescribed (ϕ=0) or have open circuit condition with D_x=0.

3. Generalized EKM solution

These are eleven $\mathbf{X}=\left[u\ \ v\ \ w\ \ \sigma_x\ \ \sigma_z\ \ \tau_{xy}\ \ \tau_{yz}\ \ \tau_{zx}\ \ \phi\ \ D_x\ \ D_z\right]^T$ primary field variables which

are to be solved. Employing multi-field multi-term EKM, the field variables for the k^{th} lamina are expressed as:

$$X_l(\xi,\zeta)=\sum_{i=1}^{n} f_l^{\,i}(\xi)g_l^i(\zeta)\cos(\omega t) \quad \text{for} \quad l=1,2,...11 \tag{18}$$

where $g_l^i(\zeta)$ and $f_l^i(\xi)$ are the unknown functions of ζ and ξ, respectively. Here, n represents the number of terms in solution. The functions $g_l^i(\zeta)$ are dependent on the k^{th} layer, while $f_l^i(\xi)$ functions are valid for all layers. These unknown functions of ζ and ξ are to be solved in two iterative steps by satisfying all homogenous support conditions.

3.1 First iterative step - solving functions $g_l^i(\zeta)$

A nice feature of EKM, not shared by many other approximation methods, is that the initial trial functions need not satisfy the essential (displacement) and nor the natural (stress) boundary conditions. The bad quality of trail function can at most lead to one or two more iteration steps (Kerr 1969, Kerr and Alexander 1968). By taking advantage of this feature, functions $f_l^i(\xi)$, along ξ direction, are assumed in the trigonometric form ($\cos i\pi\xi$ or $\sin i\pi\xi$) which actually correspond to simply-supported boundary condition. The following trial functions $f_l^i(\xi)$, along ξ -direction, are assumed for the first (Initial) step,

$$f_1^i(\xi)=f_2^i(\xi)=f_7^i(\xi)=f_8^i(\xi)=f_{10}^{\,i}(\xi)=\cos i\pi\xi$$
$$f_3^i(\xi)=f_4^i(\xi)=f_5^i(\xi)=f_6^i(\xi)=f_9^i(\xi)=f_{11}^i(\xi)=\sin i\pi\xi$$

The functions $g_l^i(\zeta)$ are to be solved in this step for which variation δX_l is given by

$$\delta X_l(\xi,\zeta)=\sum_{i=1}^{n} f_l^{\,i}(\xi)\delta g_l^i \quad \cos(\omega t) \text{ for} \qquad l=1,2,\ldots 11 \tag{19}$$

Functions $g_l^i(\zeta)$ are segregated into two-column vectors $\bar{\mathbf{G}}$ and $\hat{\mathbf{G}}$. Where $\bar{\mathbf{G}}$ contains those particular eight $8n$ primary variables which are specified at the support and interface conditions along the z-direction, and $\hat{\mathbf{G}}$ contains the remaining $3n$ dependent variables:

$$\begin{aligned}\bar{G}&=\left[\,g_1^1\ldots g_1^n \quad g_2^1\ldots g_2^n \quad g_3^1\ldots g_3^n \quad g_5^1\ldots g_5^n \quad g_7^1\ldots g_7^n \quad g_8^1\ldots g_8^n \quad g_9^1\ldots g_9^n \quad g_{11}^1\ldots g_{11}^n\,\right]^T\\ \hat{G}&=\left[\,g_4^1\ldots g_4^n \quad g_6^1\ldots g_6^n \quad g_{10}^1\ldots g_{10}^n\,\right]^T\end{aligned} \tag{20}$$

Eqs. (18) and (19) are substituted into Eq. (15). Since the $\delta f_l^{\,i}$ are known functions integration along x-direction are evaluated. Since variations for δg_l^i are arbitrary, the coefficients of δg_l^i must vanish (equal to zero) which generates the following set of $8n$ first-order ODEs and $3n$ linear algebraic equations for each layer:

$$\mathbf{M}\bar{\mathbf{G}}_{,\zeta}=\bar{\mathbf{A}}\bar{\mathbf{G}}+\hat{\mathbf{A}}\hat{\mathbf{G}} \tag{21}$$

$$\mathbf{K}\hat{\mathbf{G}}=\tilde{\mathbf{A}}\bar{\mathbf{G}} \tag{22}$$

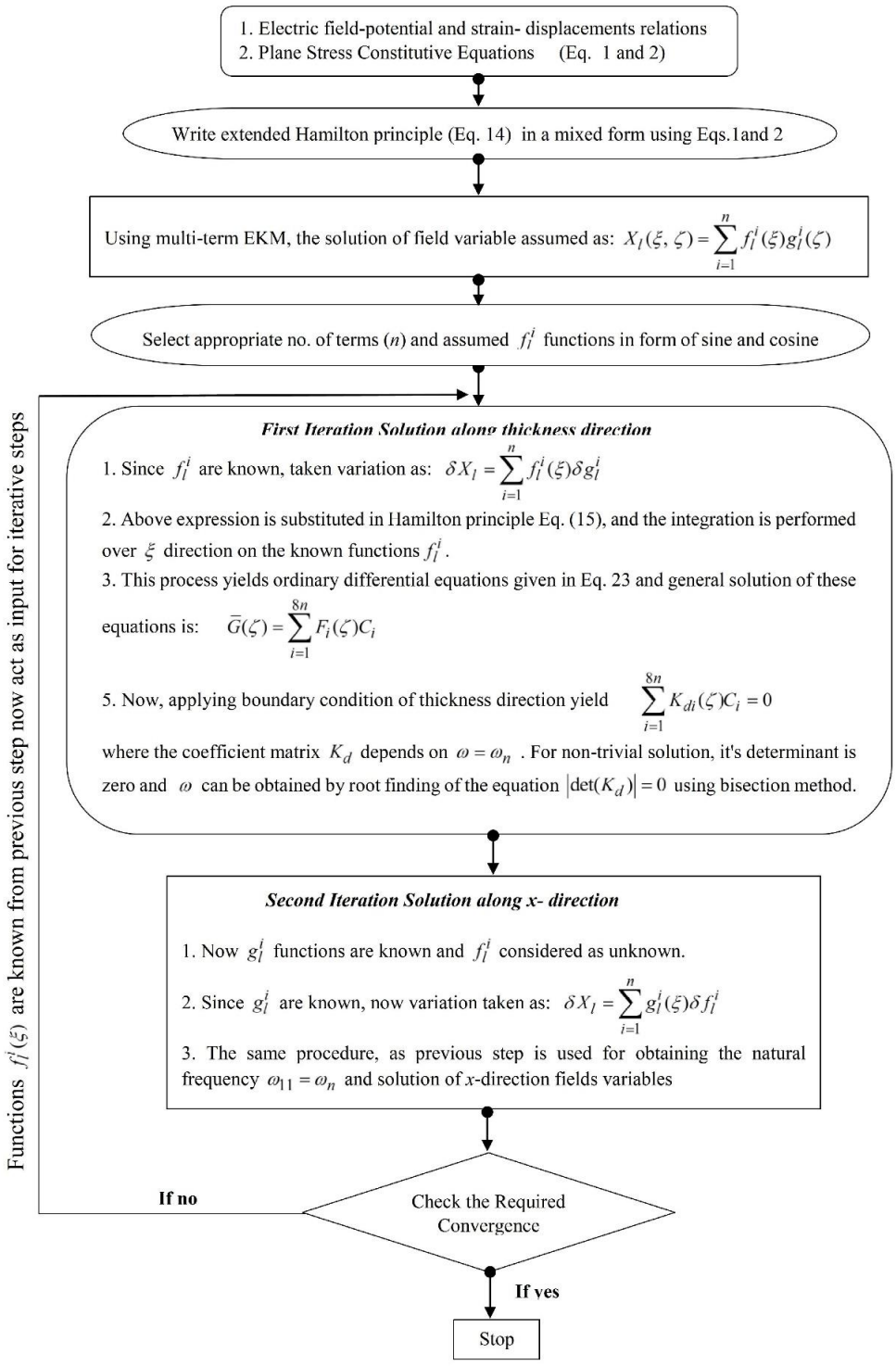

Fig. 2 Flow Chart of EKM approach for natural frequency extraction

Where $\mathbf{M}_{8n\times 8n}$, $\bar{\mathbf{A}}_{8n\times 8n}$, $\hat{\mathbf{A}}_{8n\times 3n}$, $\mathbf{K}_{3n\times 3n}$ and $\tilde{\mathbf{A}}_{3n\times 8n}$ are known matrices. Appendix A contains non-zero elements of these matrices.

The algebraic Eq. (22) is solved to obtain $\hat{\mathbf{G}}$ and put into Eq. (21) which yields a set of 8*n* first-order homogeneous ODEs as:

$$\bar{\mathbf{G}}_{,\zeta} = \mathbf{A}(\omega)\bar{\mathbf{G}} \tag{23}$$

with $\mathbf{A} = \mathbf{M}^{-1}[\bar{\mathbf{A}} + \hat{\mathbf{A}}\mathbf{K}^{-1}\tilde{\mathbf{A}}]$. Above Eq. (23) represent a system of 8*n* homogeneous first-order ODEs with constant coefficient. The general solution of Eq. (23) is obtained by applying the approach given in Kumari and Behera (2017b). The solution of Eq. (23) can be assumed in the form $\bar{\mathbf{G}}_{\mathbf{c}}(\zeta) = e^{\lambda\zeta}\mathbf{Y}$, which on substitution in Eq. (23) yields an eigenvalue problem

$$\mathbf{AY} = \lambda\mathbf{Y} \tag{24}$$

Hence the exponent λ and **Y** are the 8*n* eigenvalue and eigenvector pairs of matrix **A** and function of ω. The eigenvalues λ can be either real or occur in complex conjugate pairs. The general solution of Eq. (24) is

$$\bar{\mathbf{G}}(\zeta) = \sum_{i=1}^{8n} \mathbf{F}_i(\zeta,\omega)C_i \tag{25}$$

where $\mathbf{F}_i(\zeta,\omega)$ are column vector of functions corresponding to the eigenpairs λ_i and Y*i*. After applying the traction free boundary condition at the top and bottom of the panel and satisfying the interface continuity conditions, equation Eq. (25) yields

$$\sum_{i=1}^{8n} \mathbf{K}_{\mathbf{d}i}(\zeta,\omega)C_i = \mathbf{0} \tag{26}$$

where, the coefficient matrix $\mathbf{K}_\mathrm{d}$ depends on $\omega = \omega_n$. For nontrivial solution, it's determinant should be zero and ω can be obtained by finding roots of the equation $|det(\mathbf{K}_\mathbf{d})| = 0$ using bisection method, as discussed in Kumari and Behera (2017b), Behera and Kumari (2019). Now frequency $\omega_{01}(\omega_{01} = \omega_n)$ is known. Flow chart of solution techniques is shown in Fig. 2.

3.2 Second iterative step - solving functions $f_l^i(\xi)$

Now $\boldsymbol{g_l^i(\zeta)}$ is known from the first step and arbitrary variation is considered along the *x*-direction. Therefore, variation for this case is written as:

$$\delta X_l(\xi,\zeta) = \sum_{i=1}^{n} g_l^i(\zeta)\delta f_l^i \cos(\omega t) \quad \text{for} \quad l = 1,2,...,11 \tag{27}$$

Similarly, like the first step, $f_l^i(\xi)$ are segregated into two-column vectors $\bar{\mathbf{F}}$ and $\hat{\mathbf{F}}$. Where $\bar{\mathbf{F}}$ carries those particular 8*n* primary variables which come in the support conditions at edges *x*=0,1 and $\hat{\mathbf{F}}$ contains the remaining 3*n* variables.

$$\begin{aligned}\bar{\mathbf{F}} &= \left[f_1^1 \cdots f_1^n \quad f_2^1 \cdots f_2^n \quad f_3^1 \cdots f_3^n \quad f_4^1 \cdots f_4^n \quad f_6^1 \cdots f_6^n \quad f_8^1 \cdots f_8^n \quad f_9^1 \cdots f_9^n \quad f_{10}^1 \cdots f_{10}^n \right] \\ \hat{\mathbf{F}} &= \left[f_5^1 \cdots f_5^n \quad f_7^1 \cdots f_7^n \quad f_{11}^1 \cdots f_{11}^n \right]\end{aligned} \tag{28}$$

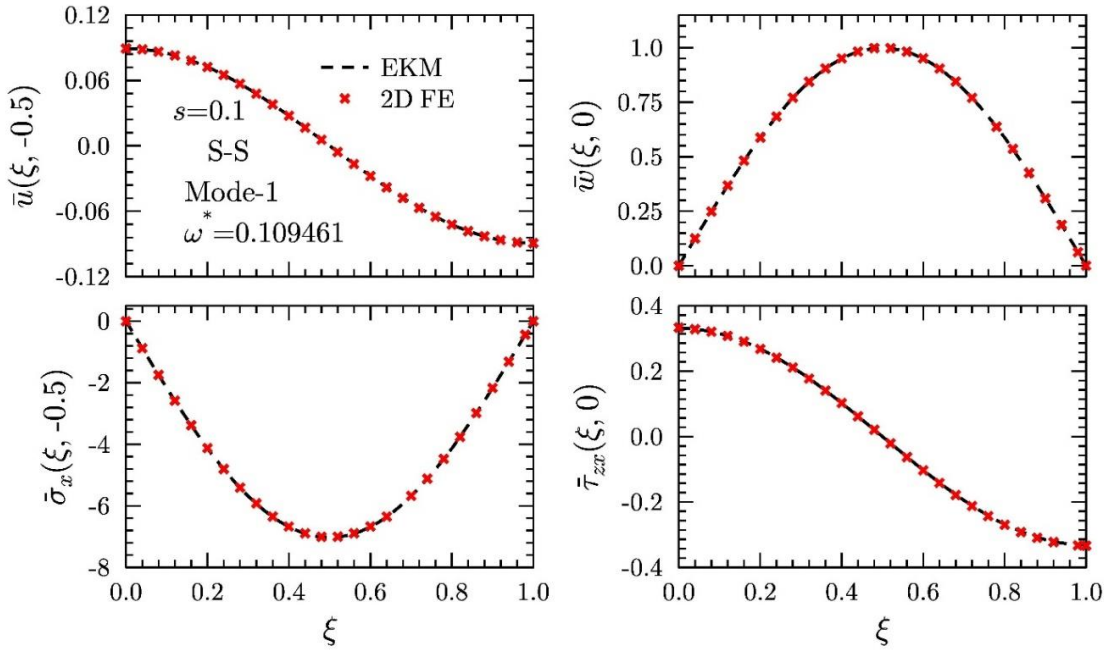

Fig. 3 Longitudinal variations of displacements and stresses for first mode of cross-ply panel [0/90/0/90^0] under S–S boundary condition

Substitute Eqs. (18) and Eq. (27) in Eq. (16), this time, integrations are evaluated along ζ-direction. Since variations δf_l^i are arbitrary, their coefficients equated to zero individually which generates the following system of 11n governing differential-algebraic equations:

$$\mathbf{N}\bar{\mathbf{F}}_{,\xi} = \bar{\mathbf{B}}\bar{\mathbf{F}} + \hat{\mathbf{B}}\hat{\mathbf{F}} \tag{29}$$

$$\mathbf{L}\hat{\mathbf{F}} = \tilde{\mathbf{B}}\bar{\mathbf{F}} \tag{30}$$

Where $\mathbf{N}_{8n\times 8n}, \bar{\mathbf{B}}_{8n\times 8n}, \hat{\mathbf{B}}_{8n\times 3n}, \mathbf{L}_{3n\times 3n}$ and $\tilde{\mathbf{B}}_{3n\times 8n}$ are known matrices. Appendix B contains nonzero terms of these matrices. Equations (29) and (30) are of the same type as Eqs. (21) and (22), and are solved in a similar fashion as mentioned in the previous step. These two-steps, one along z-direction (Sec. 3.1) and other along x-direction (Sec. 3.2) completed one iteration. These iteration steps have been continued until the desired level of accuracy achieved.

The flow chart of the iterative procedure of multi-term extended Kantorovich method is shown in Fig. 2.

4. Results and discussions

The natural frequencies are presented for three type panels such as (a) laminated elastic panels, (b) hybrid soft-core sandwich panels and (c) hybrid piezoelectric panel under different boundary conditions, and both cross-ply and angle-ply lay-ups are considered for the present study. The modal displacements, stresses, and electrical state variables are non-dimensionalized as:

$$(\bar{u},\ \bar{v},\ \bar{w}) = (u,\ v,\ w) / \max(u,\ v,\ w)$$
$$(\bar{\sigma}_x,\ \bar{\sigma}_y,\ \bar{\sigma}_z,\ \bar{\tau}_{zx},\ \bar{\tau}_{yz}) = (\sigma_x,\ \sigma_y,\ \sigma_z,\ \tau_{zx},\ \tau_{yz})\ h / (sY_0 \max(u,v,w))$$
$$\bar{D}_x = D_x h / (d_0 sY_0 \max(u,v,w)) \qquad \bar{\phi} = \phi d_0 / \max(u,v,w)$$

where (s=h/a) denotes the thickness-to-span ratio and max (u, v, w) denote the largest value of u, v and w along the thickness of panel for a particular vibration mode. The length of all panels are assumed equal to unity (a=1) for all cases and thickness of panels are taken according to the thickness to span ratio (s=h/a). For s = 0.2,0.1,0.05 the value of h are 0.2, 0.1, 0.05, respectively. In the subsequent sections, results are obtained by taking n=1, iter.2 for S-S boundary condition and n=1, iter.3 for other boundary conditions.

4.1 Laminated elastic panel

In this section, the notation system is followed to denote the stacking sequence from the bottom of the laminate to the top of the laminate. Each ply has been assumed of the same thickness and density. Angle (θ) denotes the orientation of the unidirectional fibers which is measured counterclockwise from the x-axis to fiber. The typical material properties (Chen and Lee 2004), $E_L / E_T = 25$, $G_{LT} / E_T = 0.5$, $G_{TT} / E_T = 0.2$, $\nu_{LT} = \nu_{TT} = 0.25$ are considered for lamina. Here, E represents Young's modulus, G represents the shear modulus, v represents the Poisson's ratio and subscripts L and T indicate in-plane and transverse directions, respectively. The natural frequency ω is non-dimensionalized as $\omega^* = \omega h\sqrt{\rho/G_{12}}$. Here ρ and G_{12} are the material properties of the orthotropic ply. The density of material is considered as unity.

4.1.1 Cross-ply laminated panels

In Tables 1 and 2 dimensionless natural frequencies $\omega^* = \omega h\sqrt{\rho/G_{12}}$ for cross-ply laminated panels are compared with Chen and Lee (2004) solution, which is based on a semi-analytical method known as SSDQM. In Table 1, results are compared for moderately thick laminate (s=0.1) with lay-up [0/90/0/90^0] and subjected to simply supported condition. Present results are in agreement with up to 6 digits. Further, Table 2 presents the comparison of dimensionless natural frequencies for thin (s=0.05), moderately thick (s=0.1) and thick panels (s=0.2) of different lay-ups and subjected to C-C and C-F boundary conditions. It is found that the present numerical results match excellently.

Table 1 Dimensionless natural frequencies $\omega^* = \omega h\sqrt{\rho/G_{12}}$ for S–S laminate of [0/90/0/90^0] (s=0.1)

m	3D †	SSDQM†	Present
1	0.109461	0.109461	0.109461
2	0.316561	0.316572	0.316562
3	0.542971	0.542968	0.542970
4	0.779708	0.779632	0.779708
5	1.02465	1.02682	1.024654
6	1.27545	1.25305	1.275448

†(Chen and Lee 2004)

Table 2 Dimensionless natural frequencies $\omega^* = \omega h\sqrt{\rho/G_{12}}$ for C–C and C–F laminates

B.C.	*s*		[0/90^0]	[0/90/0^0]	[0/90/0/90^0]	[(0/90)$_2$0^0]
	0.05	Present	0.0457601	0.0784461	0.0596918	0.0754865
		SSDQM†	0.0458420	0.0791464	0.0601057	0.0758616
C–C	0.1	Present	0.152817	0.202579	0.166872	0.197420
		SSDQM†	0.153462	0.205606	0.169593	0.200086
	0.2	Present	0.414520	0.470025	0.405018	0.449336
		SSDQM†	0.417144	0.474495	0.410782	0.455344
	0.05	Present	0.00771818	0.01681093	0.01154415	0.01546987
		SSDQM†	0.00771633	0.01682680	0.01154820	0.01547340
C–F	0.1	Present	0.0301246	0.0594961	0.0427713	0.0559596
		SSDQM	0.0301118	0.0598960	0.0429367	0.0561013
	0.2	Present	0.110283	0.174933	0.136844	0.169861
		SSDQM†	0.110421	0.179206	0.139518	0.172043

†(Chen and Lee, 2004)

Table 3 First five dimensionless natural frequencies $\omega^* = \omega h\sqrt{\rho/G_{12}}$ for C–C and C–F laminates

		[0/90^0]		[0/90/0^0]		[0/90/0/90^0]	
s	m	C–C	C–F	C–C	C–F	C–C	C–F
	1	0.0457601	0.0077182	0.0784461	0.0168109	0.0596918	0.0115442
	2	0.1162720	0.0460645	0.1725348	0.0849709	0.1375584	0.0628576
0.05	3	0.2084625	0.1207399	0.2837096	0.1940248	0.2309489	0.1504419
	4	0.3142542	0.2174756	0.4031675	0.3135859	0.3335674	0.2512594
	5	0.4300447	0.3285306	0.5283360	0.4390850	0.4418569	0.3589981
	1	0.1528171	0.0301246	0.2025790	0.0594961	0.1668715	0.0427713
	2	0.3460043	0.1602460	0.4172665	0.2347354	0.3507306	0.1867837
0.1	3	0.5731397	0.3774182	0.6680702	0.4906176	0.5673811	0.4027313
	4	0.8161667	0.6199417	0.9299897	0.7510733	0.7984438	0.6278359
	5	1.0670552	0.7586124	1.2025426	1.0236035	1.0363795	0.8817480
	1	0.4145196	0.1102826	0.4700252	0.1749326	0.4050183	0.1368444
	2	0.8415532	0.4562643	0.9460184	0.5731355	0.8179189	0.4683926
0.2	3	1.3340277	0.9615521	1.4900776	1.1378253	1.2981462	0.9509511
	4	1.8106346	1.4937885	2.0413664	1.6890179	1.7984837	1.5471892
	5	2.3185296	1.9623062	2.5410816	2.3248370	2.2403915	1.8859839

with results of Chen and Lee (2004) for all type of support conditions. Even for thick laminate (*s*=0.2), the present analytical model provides an excellent estimate of the fundamental natural frequency. In most of the literature work, irrespective of numerical or semi-analytical approach, only first natural frequency is reported for different boundary conditions other than the simply-supported case. Therefore, Table 3 presents the first five natural frequency parameters for thin to

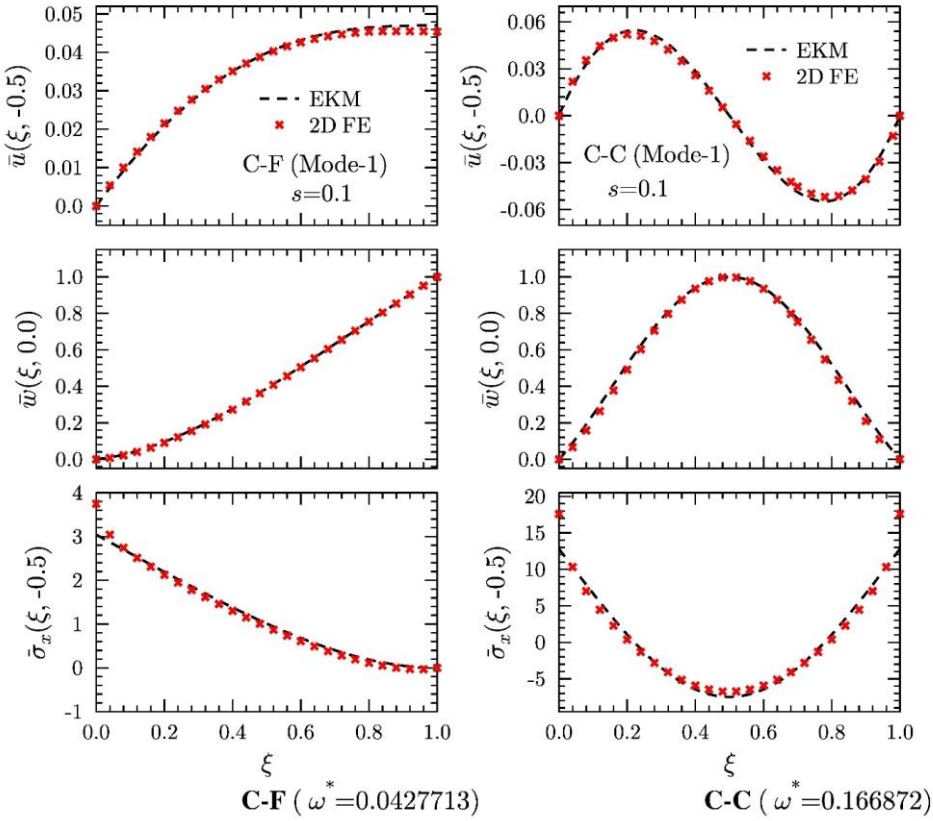

Fig. 4 Longitudinal variations of displacements and stresses for first mode of cross-ply panel [0/90/0/90^0] subjected to C–F and C–C boundary conditions

Table 4 Comparison of dimensionless natural frequencies $\omega^* = \omega h\sqrt{\rho/G_{12}}$ for S–S angle-ply laminate (s=0.1)

Configuration	m	Present	3D exact†	PSDPT$_{ds}$†
45/ − 45^0	1	0.066379	0.065634	0.065839
	2	0.23416	0.23545	0.23808
	3	0.46000	0.46217	0.47222
	4	0.71100	0.71412	0.73782
45/ −45/45^0	1	0.092192	0.091114	0.092959
	2	0.27925	0.27537	0.28489
	3	0.49046	0.48913	0.50487
	4	0.71144	0.72074	0.73951

†(Messina and Soldatos 2002)

thick (s=0.05, 0.1, 0.2) cross-ply panels having different lay-ups and under C–F and C–C boundary conditions. Where ‘m’ represent the bending mode sequence. In Fig. 3, the longitudinal variation (along x-direction) of field variables (u, w, σ_x and τ_{zx}) are presented for the first mode of cross-ply panel (s=0.1) having lay-up [0/90/0/90^0] and subjected to simply-supported (S–S) condition.

Table 5 Comparison of dimensionless natural frequencies $\omega^* = \omega h\sqrt{\rho/G_{12}}$ for different ply angle s=0.1, S–S

	$[\theta/-\theta/\theta^0]$		
θ	Present	3D exact†	PSDPT$_{ds}$†
0	0.164886	0.16489	0.16484
15	0.152843	0.15232	0.15330
30	0.125100	0.12396	0.12636
45	0.092192	0.091114	0.092959
60	0.060293	0.059879	0.060344
75	0.041737	0.041722	0.041754
90	0.039250	0.039250	0.039235

†(Messina and Soldatos 2002)

Table 6 Comparison of dimensionless natural frequencies $\omega^* = \omega\frac{a^2}{h}\sqrt{\rho/E_2}$ for different ply angle s=0.1 S–S

		$[\theta/-\theta^0]$		$[\theta/-\theta/\theta/-\theta^0]$	
θ		C–C	C–F	C–C	C–F
	Present	14.4203	2.97239	15.7292	4.01342
15	CLT†	14.2230	3.05380	16.2500	4.04350
	Abaqus*	14.5190	3.09189	15.8540	4.03148
	Present	11.7070	2.29876	13.2954	3.26705
30	CLT†	11.6720	2.28480	14.4310	3.32970
	Abaqus*	11.8525	2.33169	13.4583	3.30162
	Present	9.2124	1.67596	10.6032	2.35937
45	CLT†	9.1494	1.67770	11.5560	2.38050
	Abaqus*	9.2904	1.68266	10.7258	2.33436
	Present	7.0486	1.23340	7.8612	1.50664
60	CLT†	6.9406	1.22520	8.1679	1.49750
	Abaqus*	7.0909	1.23015	7.9344	1.61956
	Present	5.9432	1.03270	6.0567	1.05995
75	CLT†	5.9687	1.03020	6.1019	1.05600
	Abaqus*	5.9590	1.03222	6.0534	1.05812

†(Khdeir 2001)
*(Abaqus 2013)

Similarly for C–F and C–C boundary conditions, the longitudinal variation of field variables (u, w and σ_x) are plotted in Fig. 4 for the first mode of the cross-ply panel (s=0.1) with configuration [0/90/0/90^0]. Converge results of single term EKM are presented for both cases which are in excellent agreement with 2D FE results for all boundary conditions.

Table 7 Benchmarks dimensionless natural frequencies $\omega^* = \omega h\sqrt{\rho/G_{12}}$ for C–C laminate

s	m	$[45/-45^0]$	$[45/-45/45^0]$	$[(45/-45^0)_2]$	$[(45/-45)_2 0^0]$
	1	0.0363552	0.0502127	0.0489102	0.0519872
	2	0.0965222	0.1188364	0.1187872	0.1246445
0.05	3	0.1770408	0.2037139	0.2054902	0.2142898
	4	0.2733247	0.2980169	0.3032272	0.3134732
	5	0.3644464	0.3984794	0.4041575	0.4184446
	1	0.1302833	0.1480611	0.1499519	0.1555493
	2	0.2989435	0.3207747	0.3257443	0.3336526
0.1	3	0.5217359	0.5278892	0.5310994	0.5414939
	4	0.7518058	0.7541789	0.7542128	0.7616162
	5	0.9844086	1.0126406	0.9656703	0.9905958
	1	0.3830465	0.3807482	0.3817375	0.3854501
	2	0.8062149	0.7853354	0.7805780	0.7806968
0.2	3	1.2891858	1.2180621	1.2340541	1.2407574
	4	1.7949425	1.6099068	1.6730938	1.6794239
	5	2.2894534	2.2575204	2.2379873	2.1996055

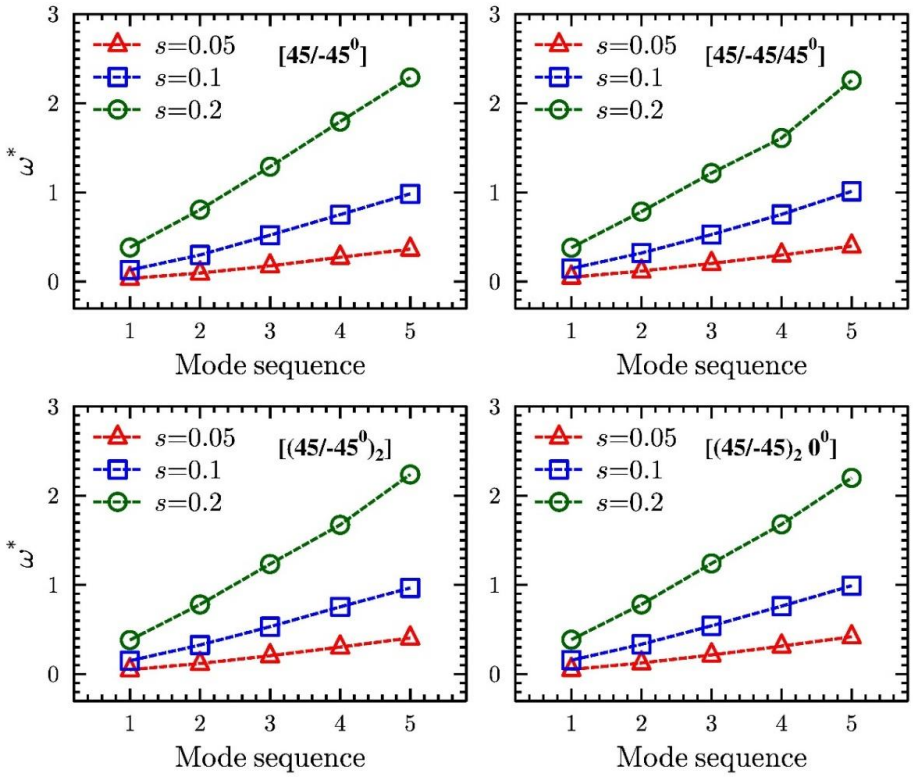

Fig. 5 Effect of thickness to span ratio (*s*) on frequency parameter for various panels subjected to C–C boundary condition

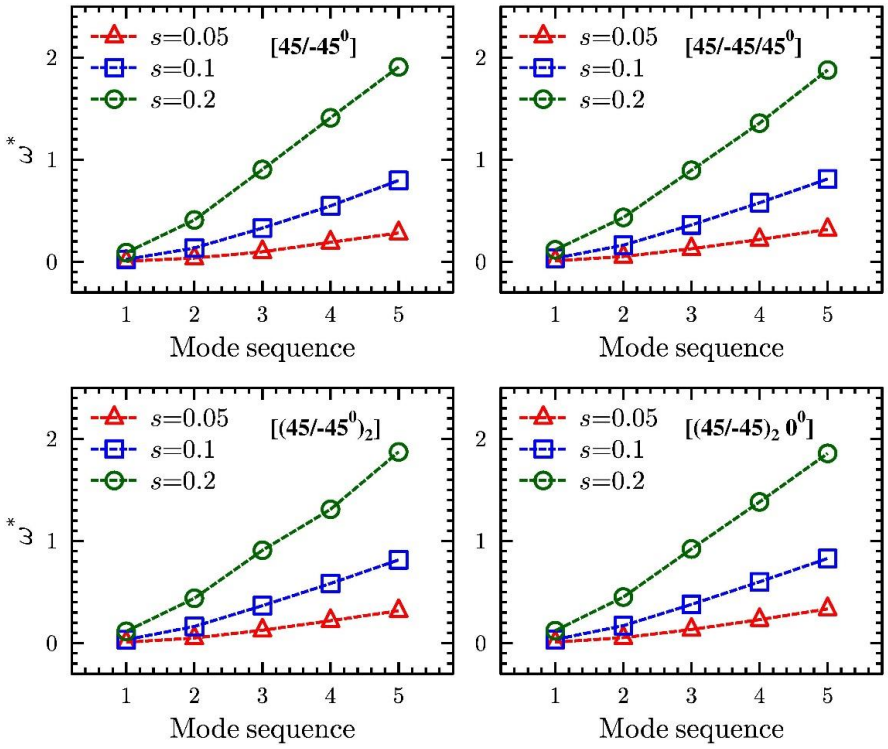

Fig. 6 Effect of thickness to span ratio (s) on frequency parameter for various panels subjected to C–F boundary condition

4.1.2 Angle-ply laminated panels

For angle-ply laminated panels, the efficacy and accuracy of the present model have been verified by comparing the fundamental frequency parameters $\omega^* = \omega h\sqrt{\rho/G_{12}}$ for the simply-supported case with Messina and Soldatos (2002) results which are based on parabolic shear deformable plate theory (PSDPT), as listed in Tables 4 and 5. Three dimensional (3D) exact results are also directly cited from the Messina and Soldatos (2002). Table 4 presents the comparison of fundamental frequency parameters, that correspond to bending vibrational modes, for two-layered antisymmetric ($45/-45^0$) and three-layered symmetric ($45/-45/45^0$) laminated panels. Similarly, Table 5 presents the comparison of the first fundamental frequency parameters for three-layered (θ /-θ / θ^0) laminated panel by considering different lamination angles. It is found that the present numerical results match exceptionally well with the results of Messina and Soldatos (2002). In case of higher bending vibrational modes, it has been observed that the present analytical model is more accurate and close to the 3D exact solution for both antisymmetric and symmetric cases. For other boundary conditions, the 3D analytical or semi-analytical solution does not exist in literature.

Therefore, for other support conditions, the reliability and accuracy of the present analytical model have been verified by comparing the fundamental frequency parameters with 3D FE results and Khdeir (2001) solution which was based on classical plate theory (CLT). For angle-ply panels, FE software ABAQUS (Abaqus, 2013) is utilized to obtain 3D FE results. The generalized plane strain conditions are simulated by creating a model of the plate with length (b) to span (a) ratio of

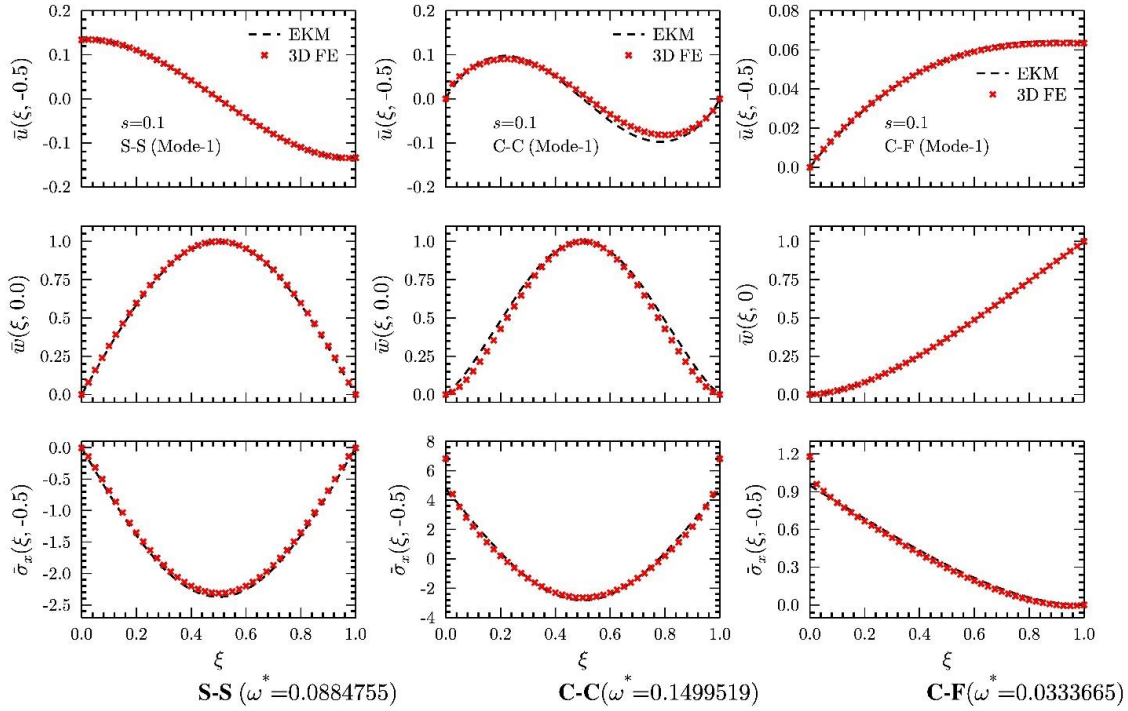

Fig. 7 Longitudinal variations of displacements and stresses for first mode of angle-ply subjected to S-S, C–C and C–F boundary conditions

20. A mesh size of 40 (*a*) × 50 (*b*) × 16 (*h*) with quadratic serendipity hexahedral element (C3D20R) under reduced integration is used for the composite panel. Before obtaining results, It was verified that the larger value of *b*/*a* did not alter the numerical results. The comparison of present results with CLT (Khdeir 2001) and 3D FE are present in Table 6 for different ply-angles. It is found that present results are in good agreement with 3D FE and CLT (Khdeir 2001) results. The present 3D elasticity solution technique gives more accurate results as compare to CLT, which is quite obvious. Benchmark natural frequencies correspond to first five bending modes are tabulated (first time) in Tables 7 and 8 for C–C and C–F boundary conditions, respectively. The results are presented for various symmetric and antisymmetric configurations and effect of thickness-to-span (^{S}) ratio on the fundamental frequencies are also studied by considering three values of *s*=0.05, 0.1, 0.2. The similar trends in frequencies have been observed for thin (^{S}=0.05) and moderate thick panel (^{S}=0.1) for all configuration and boundary conditions. But for thick panel (^{S}=0.2), the trend is slightly dissimilar for different configurations. It is also observed that an increase in laminate thickness increases the bending fundamental frequency significantly for both the cases (C–F and C–C). It has been observed that the percentage increment in the frequency is more at the higher bending modes and it is more pronounced for the thick panel, which can also be observed from Figs. 5 and 6. The non-dimensionalized frequencies parameters are plotted in Figs. 5 and 6 for different span ratio (*s*= 0.05, 0.1, 0.2) under C–C and C–F boundary conditions, respectively. The first fundamental frequency parameter for angle-ply panels, having highly heterogenous lay-up, is presented in Table 9 for different boundary conditions. The results are

Table 8 Benchmarks dimensionless natural frequencies $\omega^* = \omega h\sqrt{\rho/G_{12}}$ for C–F laminate

s	m	[45/ − 45^0]	[45/ − 45/45^0]	[(45/ − 45^0)$_2$]	[(45/ − 45)$_2$0^0]
0.05	1	0.0060335	0.0093701	0.0087129	0.0094181
	2	0.0369329	0.0522771	0.0502343	0.0536768
	3	0.0985774	0.1280457	0.1263794	0.1335488
	4	0.1915312	0.2184769	0.2192084	0.2297676
	5	0.2823315	0.3171628	0.3168461	0.3350389
0.1	1	0.0237017	0.0352313	0.0333665	0.0358267
	2	0.1358841	0.1629924	0.1631154	0.1708002
	3	0.3306276	0.3614645	0.3666264	0.3793105
	4	0.5479286	0.5781347	0.5837534	0.6002771
	5	0.7970706	0.8118251	0.8152206	0.8293952
0.2	1	0.0903066	0.1176088	0.1157008	0.1221558
	2	0.4096931	0.4344277	0.4389391	0.4509893
	3	0.9045084	0.8965775	0.9090225	0.9219428
	4	1.4104348	1.3580523	1.3098672	1.3825748
	5	1.9085943	1.8777136	1.8722491	1.8579033

Table 9 Dimensionless natural frequencies $\omega^* = \omega h\sqrt{\rho/G_{12}}$ for general lay-up angle-ply panel

s	BC	[−15/45/ − 15^0]	[−45/15/0/30/75^0]
0.05	S–S	0.0430342	0.0216779
	C–C	0.0775099	0.0460341
	C–F	0.0159608	0.0077752
0.1	S–S	0.1440320	0.0822173
	C–C	0.2054173	0.1466186
	C–F	0.0575663	0.0303379
0.2	S–S	0.3961931	0.2788671
	C–C	0.4814271	0.4143504
	C–F	0.1749444	0.1106554

tabulated (Table 9) for three-layered and five-layered panels with lay-up [−15/45/−15^0] and [−45/15/0/30/75^0], respectively. First time, benchmark results are presented for general lay-up panels subjected to general boundary conditions. These benchmark results for angle-ply panels could be used for assessing 2D numerical solutions or one-dimensional (1D) theories. In Fig. 7, the longitudinal variation of field variables (u, w, and σ_x) are presented for the first mode of the angle-ply panel (s=0.1) having lay-up [(45/−45^0)$_2$] and subjected to S–S, C–C and C–F boundary conditions. For angle-ply cases also, present EKM results match excellently with the 3D FE results.

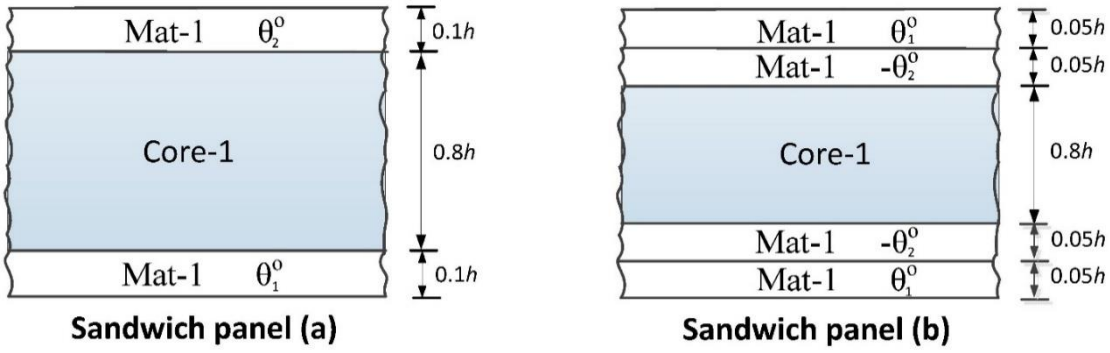

Fig. 8 Configurations of the sandwich panels

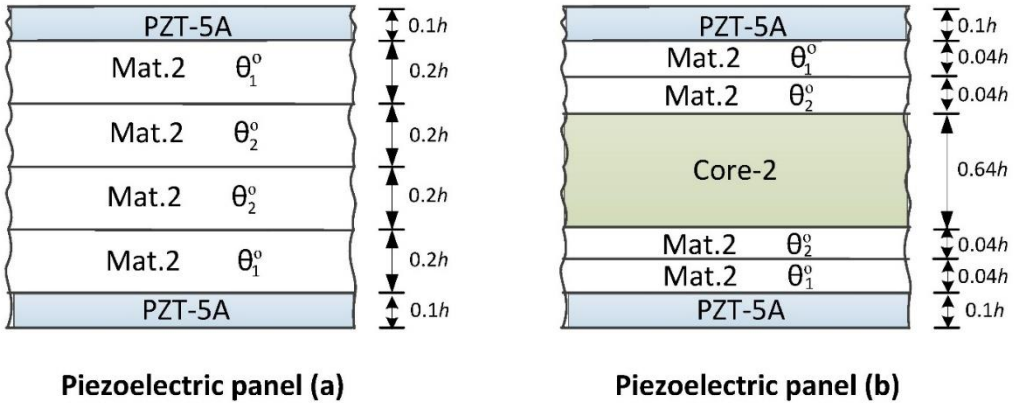

Fig. 9 Configurations of the piezoelectric-laminated panels

Table 10 Material properties for sandwich panel

Mat.1	Y_1	Y_2	Y_3	$G23$	$G13$	$G12$	$v12$	$v13$	$v23$
Gr/Ep (Kim, 2007)	172.4	6.9	6.9	1.38	3.45	3.45	0.25	0.25	0.25
Core (Kim, 2007)	0.1	0.1	0.1	0.04	0.04	0.04	0.25	0.25	0.25

Units: Young's moduli Y_i and shear moduli G_{ij} in GPa

4.2 Sandwich panels

In this section, the present method is accessed for the sandwich panel having the cross-ply and angle-ply stacking sequence. The results are presented for three-layered and five-layered sandwich panels with lay-up [θ /Core/ θ^0] and [θ_1/ θ_2/ Core/ θ_2/ $\theta_1{}^0$], respectively, as shown in Fig. 8. Table 10 contains the material properties which are used in this section. The natural frequencies ω are non-dimensionalized as $\omega^* = \omega h\sqrt{\rho/G_{12}}$. Where ρ and G_{12} is the material property of the orthotropic ply. The density of each material is considered as unity.

Table 11 presents the first five natural frequency parameters ω^* of the three-layered panel. The natural frequency parameters are tabulated for first five bending vibrational modes under three type of boundary conditions S–S, C–C and C–F. For simply supported case, present results are

Table 11 Dimensionless natural frequencies $\omega^* = \omega h\sqrt{\rho/G_{12}}$ for three-layered sandwich panel s =0.1

Configuration	m	1	2	3	4	5
	S–S	0.0342692	0.0763462	0.1287443	0.1930133	0.2678181
		(0.033158)†	-	-	-	-
[0/Core/0^0]		(0.034068)*	-	-	-	-
	C–C	0.0394549	0.0838381	0.1418824	0.2109031	0.2878363
	C–F	0.0165047	0.0501431	0.0955755	0.1531325	0.2438995
	S–S	0.0243976	0.0638127	0.1015957	0.1478207	0.2029990
		(0.024589)†	-	-	-	-
[45/Core/-45^0]		(0.024638)*	-	-	-	-
	C–C	0.0330688	0.0671282	0.1121088	0.1630150	0.2073591
	C–F	0.0101859	0.0386711	0.0845693	0.1236272	0.1471659

†EHSDT (Kim 2007)
*3D exact (Kim 2007)

Table 12 Dimensionless natural frequencies $\omega^* = \omega h\sqrt{\rho/G_{12}}$ for five-layered sandwich panel

s	BC	[0/90/Core/90/0^0]	[30/-30/Core/30/30^0]
	S–S	0.0148570	0.0144461
0.05	C–C	0.0172911	0.0166291
	C–F	0.0065793	0.0064328
	S–S	0.0340970	0.0328182
0.1	C–C	0.0364613	0.0351654
	C–F	0.0163220	0.0160346
	S–S	0.0721566	0.0695414
0.2	C–C	0.0795376	0.0779961
	C–F	0.0368487	0.0339653

validated with existing results of Kim (2007), which are based on enhanced higher-order shear deformation theory (EHSDT). 3D exact results are also directly cited from Kim (2007). It has been found that present results are in excellent agreement with 3D exact and EHSDT results. In Table 12, benchmark natural frequencies are tabulated for five-layered sandwich panels (first time) of different thickness and subjected to different support conditions. The results for other boundary condition are also thoroughly verified with 3D FE results by utilizing the commercial FE software ABAQUS (Abaqus 2013). As the s value increases from 0.05 to 0.2 (thin to thick panel), the natural frequency increases significantly for all type of boundary conditions, which is clearly observed from Table 12.

4.3 Piezoelectric panels

4.3.1 Validation with exact results for simply-supported (S–S) case

For Piezoelectric problems, the solution method is validated with the available exact solution given by Heyliger and Brooks (1995) and Kumari *et al.* (2007) for simply-supported case. The natural frequencies compared for a single layered piezoelectric panel and a three layered cross-ply

(orthotropic) hybrid panel both having $S = l/h = 4$. The material properties for piezoelectric laminated panels, taken as (Kumari *et al.* 2007): $[(Y_1, Y_2, Y_3, G_{23}, G_{13}, G_{12}), \nu_{12}, \nu_{13}, \nu_{23}]$,

$[(e_{31}, e_{32}, e_{33}, e_{24}, e_{15}), (\varepsilon_{11}/\varepsilon_0, \varepsilon_{22}/\varepsilon_0, \varepsilon_{33}/\varepsilon_0)]=$

Material A (PZT-4): [(81.3, 81.3, 64.5, 25.6, 25.6, 30.6)GPa, 0.329, 0.432, 0.432], [(−5.20, − 5.20, 15.08, 12.72, 12.72) C/m^2, (1475, 1475, 1300)] ,

Material C: [(132.38, 10.756, 10.756, 5.6537, 3.606, 5.6537) GPa, 0.24, 0.24, 0.49], [(0, 0, 0, 0, 0) C/m^2, (3.5, 3.5, 3)],

Material D (PVDF): [(237.0, 23.2, 10.5, 2.15, 4.4, 6.43) GPa, 0.154, 0.178, 0.177], [(−0.13, −0.14, −0.28, −0.01, −0.01) C/m^2, (12.5, 11.98, 11.98)].

Where Y_i denotes Young's modulus, G_{ij} denotes shear modulus, v_{ij} denotes Poisson ratios and e_{ij} denotes piezoelectric stress constants. The density of each material is considered as a unity. Table 13 presents the first ten natural frequencies for the single-layered panel of material A, having open and closed circuit conditions at the top and bottom surfaces. Similarly, Table 14, presents the first eight natural frequencies for the three-layered hybrid panel [A(0.1 h)/C(0.8 h)/A(0.1 h)] under closed-circuit condition. The three-layered panel is a substrate of material C with two layers of material A (thickness 0.1h) bonded to the bottom and top of the substrate. It is observed that the present numerical results match exactly with the results of Heyliger and Brooks (1995) and Kumari *et al.* (2007) for both cases.

4.3.2 Validation for other boundary conditions

Since no 3D piezo-elasticity based analytical solution is available for the other boundary conditions. Therefore, present results have been validated with Shu (2005a) results which were based on an equivalent single layer theory. The present results have been also compared to Zhou *et al.* (2009) results which are based on a 2D semi-analytical method known as SS-DQM. Table 15 shows the comparison of the natural frequencies with Shu (2005a) results for three-layer cross-ply hybrid panel [A(0.1h)/C(0.8h)/A(0.1h)] under S–S, C–C and C–F boundary conditions. It is observed that present numerical results show very good agreement with Shu (2005a) results for all boundary conditions.

In tables 16-19, natural frequencies are presented for various type of piezoelectric panels subjected to the different type of mechanical and electrical boundary conditions. For such cases, first-time analytical results are tabulated because it is very difficult to derive analytical solutions based on the coupled piezo-elasticity equations (Zhou *et al.* 2009). For all the cases, the present numerical results are also compared with semi-analytical results of the Zhou *et al.* (2009). In this section, Z represents PZT-4 layer having ply angle $\theta = 0^o$ and V represent PVDF layer having ply angle $\theta = 90^o$. For all panels, each ply is assumed to have the same thickness just as given in Zhou *et al.* (2009). The mechanical boundary conditions at the top and bottom surfaces are always assumed to be traction-free, while the others are represented by notations such as C–S|EC–EO/EO–EC. In which C–S|EC–EO indicates that the laminated panel has clamped boundary condition and electrically close-circuit at x= 0, and simply-supported boundary condition and electrically open-circuit at x=a. Further, EO–EC represents electrically open-circuit and closed-circuit conditions at z= –h/2 and z=h/2, respectively.

Comparison of present results with 3D exact and SS-DQM results is presented in Table 16 for a simply-supported single-layer PZT panel (S–S|EC–EC/EC–EO) with different thickness-to-span ratio (s). The present results show excellent agreement with 3D exact and SS-DQM results of Zhou *et al.* (2009). Table 17 gives the first fundamental frequency parameters for various piezo-

Table 13 Natural frequencies ω/100 (rad/sec) for single-layered piezoelectric panel of material A under S--S boundary conditions (L/h=4)

	Closed-circuit			Open circuit		
m	Present	2D Exact†	2D Exact*	Present	2D Exact†	2D Exact*
1	52580.7492	52580.6684	52580.67	53046.7611	53046.7643	53046.76
2	234515.3381	234514.6611	234514.7	254503.0584	254503.6015	254503.6
3	560242.4709	560241.7497	560241.7	642210.6577	642210.3979	642210.4
4	969921.2367	969921.0825	969921.1	972665.6277	972665.3311	972665.4
5	1154041.3588	1154041.8570	1154042	1224773.5813	1224774.5120	1224774
6	1513041.5592	1513041.9370	1513042	1545514.4764	1545514.5710	1545515
7	2016806.6020	2016798.2430	2016798	2021618.1966	2021620.5310	2021621
8	2319010.3835	2319013.3060	2319013	2321380.5393	2321388.4520	2321388
9	2522451.7309	2522446.5400	2522449	2545885.9786	2545884.2820	2545884
10	3017992.5111	3017998.4710	3017998	3019774.5832	3019775.0540	3019775

†(Kumari *et al*. 2007)
*(Heyliger and Brooks 1995)

Table 14 Natural frequencies ω (rad/s) for three-layer piezoelectric panel [A/C/A] subjected to S-S boundary conditions (L/h=4)

m	Present	2D Exact†	2D Exact*
1	4061328.1367	4061328.914	4061328.8
2	27900175.6980	27900191.25	27900191
3	36428990.7128	36428990.71	36428990
4	37712869.7731	37712838.66	37712838
5	55899719.6294	55899719.63	55899720
6	74614977.7303	74615081.44	74615082
7	80757918.0315	80757822.1	80757823
8	102701250.1003	102701050.5	102701050

†(Kumari *et al*. 2007)
*(Heyliger and Brooks 1995)

laminated panel subjected to clamped and closed-circuit boundary conditions at the x=0 and x=a, as well as electrically closed-circuit conditions at z= $-h/2$ and z=$h/2$. The results show good agreement with SS-DQM results. From table 17 is also observed that the first fundamental frequency increases as the thickness-to-span ratio (s) of panels increase. The lay-up scheme also has a significant effect on the frequencies.

The effects of electric boundary conditions at the top and bottom surfaces of panels on the natural frequencies of piezoelectric laminated panels are studied in Table 18. The results are tabulated for various lay-up scheme of piezoelectric panels which has s = 0.1 and C–F and electrically closed boundary condition at ends (x = 0 and x = a). Similarly, in Table 19, the effects of electric boundary conditions at the two ends (x = 0 and x = l) on the natural frequencies of piezoelectric laminated panels are studied. The results are tabulated for various lay-up scheme of piezoelectric panels which has s = 0.1 and C–C and electric open boundary condition at top and

bottom surfaces ($z= -h/2$ and $z=h/2$). Due to the weak coupling between the electric and elastic fields, the effect of electric boundary condition on the natural frequencies of piezoelectric laminated panels is not very significant but these small effects are very much important to detect accurately for precise control applications. For symmetric laminates, the natural frequencies parameters for EO–EC-z and EC–EO-z are identical which is quite obvious.

Table 15 Natural frequencies ω (rad/s) for three-layer piezoelectric panel [A/C/A] subjected to various boundary conditions

		L/h=4		L/h =50	
BC		Closed	Open	Closed	Open
S–S	Present	0.4061e7	0.4062e7	0.3941e5	0.3941e5
	Shu†	0.4043e7	0.4043e7	0.3922e5	0.3922e5
	2D Exact*	0.4061e7	0.4062e7	0.3941e5	0.3941e5
C–F	Present	0.1721e7	0.1703e7	0.1409e5	0.1399e5
	Shu†	0.1728e7	0.1727e7	0.1400e5	0.1400e5
C–S	Present	0.4725e7	0.4707e7	0.6153e5	0.6112e5
	Shu†	0.4682e7	0.4680e7	0.6080e5	0.6080e5
C–C	Present	0.5556e7	0.5479e7	0.8899e5	0.8813e5
	Shu†	0.5429e7	0.5426e7	0.8740e5	0.8739e5

† (Shu, 2005a)
*(Heyliger and Brooks 1995)

Table 16 Dimensionless natural frequencies $\omega^* = \omega h\sqrt{\rho/G_{12}}$ for a PZT-4 panel (S–S|EC–EC/EC–EO)

	s=0.01	s=0.05	s=0.1	s=0.2
Present	0.00058417	0.01453587	0.05732267	0.217831236
3D Exact†	0.00058393	0.01453694	0.05740433	0.21899052
SSDQM†	0.00058394	0.01453706	0.05740478	0.21899218

†(Zhou *et al.* 2009)

Table 17 Dimensionless| natural frequency parameter $\omega^* = \omega h\sqrt{\rho/G_{12}}$ for piezoelectric laminated plate with different lay-up (C–C|EC–EC/EC–EC)

		[Z/V]	[Z/V/Z]	[Z/V/Z/V]	[Z/V/Z/V/Z]
s=0.01	Present	0.00084680	0.00125180	0.00098906	0.00111957
	SSDQM†	0.00086082	0.00131280	0.00099782	0.00122015
s=0.05	Present	0.02031843	0.02799720	0.02335348	0.02525749
	SSDQM†	0.02063014	0.02855171	0.02274281	0.02710401
s=0.1	Present	0.07343331	0.08581248	0.07256331	0.08103439
	SSDQM†	0.07453177	0.08882316	0.07527702	0.08555909
s=0.2	Present	0.23300522	0.23028151	0.20296947	0.24074441
	SSDQM†	0.23651852	0.23957155	0.21220645	0.22500977

†(Zhou *et al.* 2009)

Table 18 Dimensionless| natural frequency parameters $\omega^* = \omega h\sqrt{\rho/G_{12}}$ for piezoelectric laminated plate with different lay-up (C–F|EC–EC, s=0.1)

BC-z		[Z/V]	[Z/V/Z]	[Z/V/Z/V]	[Z/V/Z/V/Z]
EO–EO	Present	0.013220302	0.019210203	0.014742228	0.018085716
	SSDQM†	0.013192509	0.019229189	0.014949811	0.018030044
EO–EC	Present	0.013216863	0.018633168	0.014735367	0.174903612
	SSDQM†	0.013181205	0.01919484	0.014940033	0.018013882
EC–EO	Present	0.013103416	0.018633168	0.014328805	0.174903612
	SSDQM†	0.013163973	0.01919484	0.014933324	0.018013882
EC–EC	Present	0.013091886	0.018044906	0.014239077	0.016903507
	SSDQM†	0.013158104	0.019165257	0.014926037	0.018000255

†(Zhou *et al.* 2009)

Table 19 Dimensionless natural frequency parameters $\omega^* = \omega h\sqrt{\rho/G_{12}}$ for piezoelectric laminated plate with different lay-up (C–C/EO–EO, s=0.1)

BC-x		[Z/V]	[Z/V/Z]	[Z/V/Z/V]	[Z/V/Z/V/Z]
EC–EC	Present	0.07373324	0.08625497	0.07325368	0.08373173
	SSDQM†	0.07536575	0.08978304	0.07570815	0.08615817
EO–EC	Present	0.07381218	0.08625639	0.07326633	0.08372514
	SSDQM†	0.07546851	0.08977754	0.07549783	0.08556069
EO–EO	Present	0.07388739	0.08625764	0.07333423	0.08372603
	SSDQM†	0.07542978	0.08974057	0.07538146	0.08541972
EC–EO	Present	0.07381218	0.08625639	0.07326633	0.08372514
	SSDQM†	0.07546857	0.08977759	0.07549792	0.08556081

†(Zhou *et al.* 2009)

Table 20 Material constants.

Material	Y_1	Y_2	Y_3	G_{23}	G_{13}	G_{12}	ν_{12}	ν_{13}	ν_{23}	ρ
Mat. 2	181.0	10.3	10.3	2.87	7.17	7.17	0.28	0.28	0.33	1578
Core-2	0.276	0.276	3.45	0.1104	0.414	0.414	0.25	0.02	0.02	1000
PZT-5A	61.0	61.0	53.2	21.1	21.1	22.6	0.35	0.38	0.38	7600
Material	d_{13}	d_{32}	d_{33}	d_{24}	d_{15}	η_{11}	η_{22}	η_{33}		
PZT-5A	-171	-171	374	584	584	15.3	15.3	15.0		

Units: Young's moduli Y_i and shear moduli G_{ij} in GPa; density (ρ) in Kg/m^3; piezoelectric strain coefficients d_{ij} in pm/V; electric permittivities η_{ij} in nF/m; * Where $d_0 = d_{33}$ pm/V; Y_0 = 10.3 GPa

4.3.3 Some new benchmark results

In Tables 21 and 22, benchmark natural frequencies parameters, correspond to first three bending modes, are tabulated for thick (s=0.2) smart composite and sandwich piezoelectric panels subjected to various mechanical boundary conditions at ends (x= 0 and x= a), and electrically open or close boundary condition at top and bottom surfaces (z= –h/2 and z=h/2). The configurations of smart composite and sandwich panels are shown in Fig. 9, where the properties of the materials are given in Table 20.

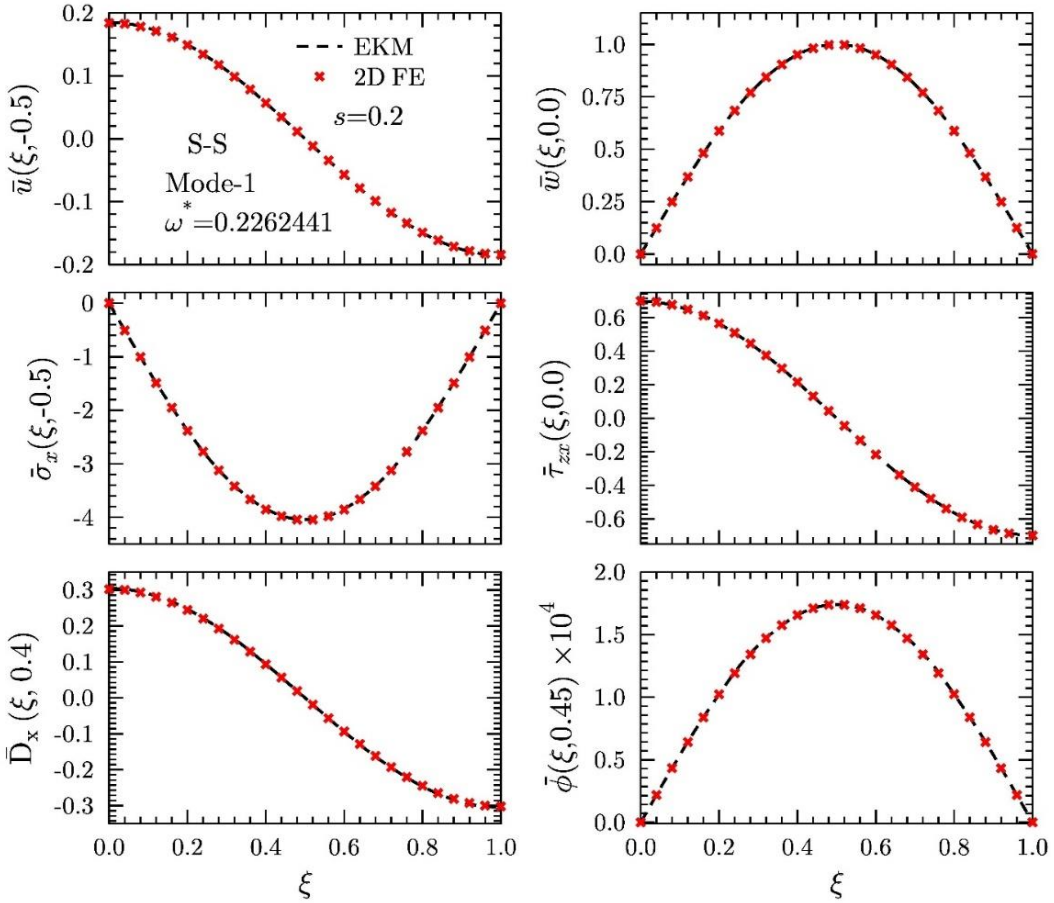

Fig. 10 Longitudinal variations of displacements, stresses and electrical variables for cross-ply piezoelectric panel with lay-up [(PZT-5A/0/90)$_2$] (EC–EC/EC–EC, s=0.2) and subjected to S-S boundary condition

Table 21 Benchmarks dimensionless natural frequencies $\omega^* = \omega h\sqrt{\rho/G_{12}}$ for piezo-electric laminated plate with different lay-up (EC–EC-x, s=0.2)

	m	[(PZT-5A/0/90)$_2$]		[(PZT-5A/30/-30)$_2$]	
		Close circuit	Open Circuit	Close circuit	Open Circuit
S–S	1	0.2262441	0.2306577	0.2273041	0.2337663
	2	0.5701732	0.5778008	0.6170847	0.6248754
	3	0.9380969	0.9502934	1.0328357	1.0504881
C–C	1	0.2961215	0.2978862	0.3254689	0.3312718
	2	0.6059094	0.6134991	0.6667578	0.6767873
	3	0.9848215	1.0024115	1.0644729	1.0774317
C–F	1	0.0952360	0.0974279	0.0916322	0.0945427
	2	0.3399906	0.3516473	0.3616073	0.3703060
	3	0.6975272	0.7073793	0.7936180	0.8036954

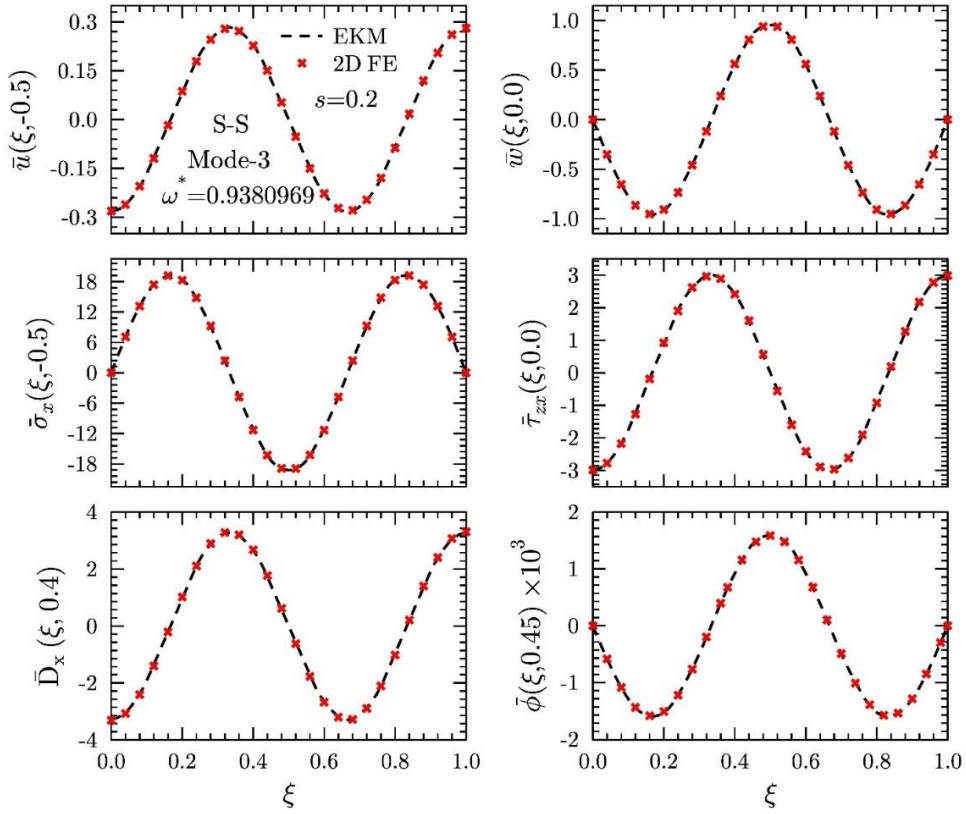

Fig. 11 Longitudinal variations of displacements, stresses and electrical variables for cross-ply piezoelectric panel with lay-up [(PZT-5A/0/90)$_2$] (EC–EC/EC–EC, s=0.2) and subjected to S-S boundary condition

The natural frequencies ω are non-dimensionalized as $\omega^* = \omega h\sqrt{\rho/G_{12}}$. Where ρ and G_{12} is the material property of the elastic ply (Mat. 2). The natural frequencies are presented for both cross-ply and angle-ply case. First time, benchmark results are presented for angle-ply piezo-laminated and piezo-sandwich panels subjected to general boundary conditions. The first three frequencies of the cross-ply and angle-ply piezo-laminated panel are tabulated in Table 21 for various type of boundary conditions i.e S–S, C–C and C–F, respectively, and with open and closed circuit conditions at the top and bottom surfaces. Similarly, the first three natural frequencies of the cross-ply and angle-ply piezo-sandwich panel are tabulated in Table 22. The numerical results of this sub-section are also thoroughly verified with 3D FE results by utilizing the commercial FE software ABAQUS (Abaqus, 2013). It is found that present results are in good agreement with 3 D FE results. It is also observed that the effect of electric boundary condition at the top and bottom surfaces (z= –h/2 and z=h/2) is more significant at higher bending mode as compared to first bending mode, for all the cases. The natural frequencies are higher for electrically open boundary conditions at the top and bottom surfaces of panels, as compared to electrically close conditions. The effect of electric boundary conditions at the top and bottom surfaces of panels is comparatively less in piezo-sandwich panels for all three bending modes. The present method can detect these effects accurately, which are very much important for precise control applications.

Table 22 Benchmarks dimensionless natural frequencies $\omega^* = \omega h\sqrt{\rho/G_{12}}$ for sandwich piezo-laminated panel with different lay-up (EC–EC-*x*, *s*=0.2)

	m	[(PZT-5A/0/90)$_2$Core]		[(PZT-5A/30/-30)$_2$Core]	
		Close circuit	Open Circuit	Close circuit	Open Circuit
S–S	1	0.1158795	0.1178767	0.115345381	0.1175675
	2	0.2649350	0.2685149	0.269836623	0.2744607
	3	0.4387201	0.4450557	0.457879817	0.4662227
C–C	1	0.1367742	0.1386386	0.140346341	0.1427526
	2	0.2806270	0.2846647	0.298404971	0.3039903
	3	0.4724557	0.4794519	0.501668413	0.5102549
C–F	1	0.0532131	0.0541403	0.052870788	0.0541787
	2	0.1674822	0.1705361	0.167115893	0.1703328
	3	0.3287606	0.3312440	0.337620828	0.3435029

In Fig. 10, the longitudinal variation of field variables ($u, w, \sigma_x, \tau_{zx}, \phi, D_x$) are presented for the first mode of the thick piezoelectric panel (a) (*s*=0.2) under to S–S boundary conditions and with closed-circuit condition. Similarly, the longitudinal variation of field variables ($u, w, \sigma_x, \tau_{zx}, \phi, D_x$) for the third mode of the thick piezoelectric panel (a) (*s*=0.2) under S–S boundary condition are plotted in Fig. 11. Converge results of single term EKM are presented for both cases which match excellently with 2D FE results for both mode shapes.

5. Conclusions

These are some novel and significant contributions of the present work:

i A 3D piezo-elasticity based analytical solution for free vibration analysis of arbitrary supported (S–S, C–C, C–F, and C–S) angle-ply elastic and piezo-laminated panel is presented for the first time.

ii The present analytical solution is applicable to thick as well as thin laminates of general configurations with arbitrary angle-ply lay-up or materials properties.

iii First time, multi-term multi-field extended Kantorovich approach in conjunction with modified Hamiltons principle is applied to derive the dynamic solution for an angle-ply smart laminated plate under cylindrical bending.

iv For extracting the natural frequencies and mode shapes of elastic and piezo-laminated panels a robust algorithm (quadruple precision FORTRAN code) is developed, which is very challenging (Heyliger and Brooks, 1995) even for simple case and configurations even when ODEs are solved in one direction, only.

v The numerical results are reported for various type of panels such as cross-ply/angle-ply elastic panels, sandwich panels and piezoelectric panels under different combination of boundary conditions and lay-up scheme. It is found that the single-term solution is sufficient enough for determining the natural frequencies accurately.

vi Accuracy and efficacy of the present method are thoroughly verified by comparing the present results with the existing solutions in literature or with the finite element model (Abaqus).

vii The present 3D analytical solution can predict the effect of electric boundary condition on the natural frequencies of piezoelectric laminated panels. Though the effect is not very significant due to the weak coupling between the electric and elastic fields. But these small effects are very much important for precise control applications.

viii This work will fill up the gap in the literature and further can be used to assess various 1D/2D theories and numerical methods.

ix In the future, this method can also be extended to the dynamic analysis of imperfect angle-ply elastic/piezoelectric laminated panels subjected to arbitrary boundary conditions.

Acknowledgments

This work was supported by funding received from Science and Engineering Research Board (SB/FTP/ETA-420/2013), India.

References

Abad, F. and Rouzegar, J. (2019), "Exact wave propagation analysis of moderately thick Levytype plate with piezoelectric layers using spectral element method", *Thin-Walled Struct.*, **141**, 319–331. https://doi.org/10.1016/j.tws.2019.04.007.

Abaqus, A. (2013), "6.13 Analysis Users Manual", *SIMULIA,* Providence, IR, USA.

Balabaev, S. and Ivina, N. (2014), "A three-dimensional analysis of natural vibrations of rectangular piezoelectric transducers", *Russian J. Nondestructive Testing*, **50**(10), 602–606. https://doi.org/10.1134/S1061830914100027.

Barati, M.R. and Zenkour, A.M. (2018), "Electro-thermoelastic vibration of plates made of porous functionally graded piezoelectric materials under various boundary conditions", *J. Vib. Control*, **24**(10), 1910–1926. https://doi.org/10.1177/1077546316672788.

Batra, R. and Liang, X. (1997), "The vibration of a rectangular laminated elastic plate with embedded piezoelectric sensors and actuators", *Comput. Struct.*, **63**(2), 203–216. https://doi.org/10.1016/S0045-7949(96)00349-5.

Behera, S. and Kumari, P. (2018), "Free vibration of Levy-type rectangular laminated plates using efficient zig-zag theory", *Adv. Comput. Design*, **3**(3), 213–232. https://doi.org/10.12989/acd.2018.3.3.213.

Behera, S. and Kumari, P. (2019), "Analytical Piezoelasticity Solution for Natural Frequencies of Levy-Type Piezolaminated Plates", *J. Appl. Mech.*, **11**(03), 1950023. https://doi.org/10.1142/S1758825119500236.

Chen, W. and Ding, H. (2002), "On free vibration of a functionally graded piezoelectric rectangular plate", *Acta Mechanica*, **153**(3-4), 207–216. https://doi.org/10.1007/BF01177452.

Chen, W. and Lee, K.Y. (2004), "On free vibration of cross-ply laminates in cylindrical bending", *J. Sound Vib.*, **3**(273), 667–676. https://doi.org/10.1016/j.jsv.2003.08.003.

Chen, W. and Lü, C. (2005), "3D free vibration analysis of cross-ply laminated plates with one pair of opposite edges simply supported", *Compos. Struct.*, **69**(1), 77–87. https://doi.org/10.1016/j.compstruct.2004.05.015.

Cheng, Z.Q. and Batra, R. (2000a), "Three-dimensional asymptotic analysis of multiple-electroded piezoelectric laminates", *AIAA J.*, **38**(2), 317–324. https://doi.org/10.2514/2.959.

Cheng, Z.Q. and Batra, R. (2000b), "Three-dimensional asymptotic scheme for piezothermoelastic laminates", *J. Thermal Stresses*, **23**(2), 95–110. https://doi.org/10.1080/014957300280470.

Cheng, Z.Q., Lim, C. and Kitipornchai, S. (1999), "Three-dimensional exact solution for inhomogeneous and laminated piezoelectric plates", *J. Eng. Sci.*, **37**(11), 1425–1439. https://doi.org/10.1016/S0020-7225(98)00125-6.

Cheng, Z.Q., Lim, C. and Kitipornchai, S. (2000), "Three-dimensional asymptotic approach to

inhomogeneous and laminated piezoelectric plates", *J. Solids Struct.*, **37**(23), 3153–3175. https://doi.org/10.1016/S0020-7683(99)00036-0.

Dube, G., Kapuria, S. and Dumir, P. (1996a), "Exact piezothermoelastic solution of simplysupported orthotropic circular cylindrical panel in cylindrical bending", *Archive Appl. Mech.*, **66**(8), 537–554. https://doi.org/10.1007/BF00808143.

Dube, G., Kapuria, S. and Dumir, P. (1996b), "Exact piezothermoelastic solution of simply supported orthotropic flat panel in cylindrical bending", *J. Mech. Sci.*, **38**(11), 1161–1177. https://doi.org/10.1016/0020-7403(96)00020-3.

Ebrahimi, F. and Barati, M.R. (2016), "Size-dependent thermal stability analysis of graded piezomagnetic nanoplates on elastic medium subjected to various thermal environments", *Appl. Phys.*, **122**(10), 910. https://doi.org/10.1007/s00339-016-0441-9.

Ebrahimi, F. and Barati, M.R. (2017a), "Damping vibration analysis of smart piezoelectric polymeric nanoplates on viscoelastic substrate based on nonlocal strain gradient theory", *Smart Mater. Struct.*, **26**(6), 065018. https://doi.org/10.1088/1361-665X/aa6eec.

Ebrahimi, F. and Barati, M.R. (2017b), "Magnetic field effects on dynamic behavior of inhomogeneous thermo-piezo-electrically actuated nanoplates", *J. Brazilian Soc. Mech. Sci. Eng.*, **39**(6), 2203–2223. https://doi.org/10.1007/s40430-016-0646-z.

Heyliger, P. and Brooks, S. (1995), "Free vibration of piezoelectric laminates in cylindrical bending", *J. Solids Struct.*, **32**(20), 2945–2960. https://doi.org/10.1016/0020-7683(94)00270-7.

Heyliger, P. and Brooks, S. (1996), "Exact solutions for laminated piezoelectric plates in cylindrical bending", *J. Appl. Mech.*, **63**(4), 903–910.

Heyliger, P. and Saravanos, D. (1995), "Exact free-vibration analysis of laminated plates with embedded piezoelectric layers", *J. Acoustical Soc. America*, **98**(3), 1547-1557. https://doi.org/10.1121/1.413420.

Hussein, M. and Heyliger, P. (1998), "Three-dimensional vibrations of layered piezoelectric cylinders", *J. Eng. Mech.*, **124**(11), 1294–1298. https://doi.org/10.1061/(ASCE)0733-9399(1998)124:11(1294).

Jones, A.T. (1970), "Exact natural frequencies for cross-ply laminates", *J. Compos. Mater.*, **4**(4), 476–491. https://doi.org/10.1177/002199837000400404.

Jones, A.T. (1971), "Exact natural frequencies and modal functions for a thick off-axis lamina", *J. Compos. Mater.*, **5**(4), 504–520. https://doi.org/10.1177/002199837100500409.

Kapuria, S. and Dhanesh, N. (2017), "Free edge stress field in smart piezoelectric composite structures and its control: An accurate multiphysics solution", *J. Solids Struct.*, **126**, 196–207. https://doi.org/10.1016/j.ijsolstr.2017.08.007.

Kapuria, S. and Kumari, P. (2011), "Extended Kantorovich method for three-dimensional elasticity solution of laminated composite structures in cylindrical bending", *J. Appl. Mech.*, **78**(6), 061004. https://doi.org/10.1115/1.4003779.

Kapuria, S. and Kumari, P. (2012), "Multiterm extended Kantorovich method for three-dimensional elasticity solution of laminated plates", *J. Appl. Mech.*, **79**(6), 061018. https://doi.org/10.1115/1.4006495.

Kapuria, S. and Kumari, P. (2013), "Extended Kantorovich method for coupled piezoelasticity solution of piezolaminated plates showing edge effects", *Proceedings of the Royal Society A: Mathematical, Physical and Engineering Sciences*, **469**(2151), 20120565. https://doi.org/10.1098/rspa.2012.0565.

Kapuria, S., Kumari, P. and Nath, J. (2010), "Efficient modeling of smart piezoelectric composite laminates: a review", *Acta Mechanica*, **214**(1-2), 31–48. https://doi.org/10.1007/s00707-010-0310-0.

Kerr, A.D. (1969), "An extended Kantorovich method for the solution of eigenvalue problems", *J. Solids Struct.*, **5**(6), 559–572. https://doi.org/10.1016/0020-7683(69)90028-6.

Kerr, A.D. and Alexander, H. (1968), "An application of the extended Kantorovich method to the stress analysis of a clamped rectangular plate", *Acta Mechanica*, **6**(2-3), 180–196. https://doi.org/10.1007/BF01170382.

Khdeir, A. (2001), "Free and forced vibration of antisymmetric angle-ply laminated plate strips in cylindrical bending", *J. Vib. Control*, **7**(6), 781–801. https://doi.org/10.1177/107754630100700602.

Kim, J.S. (2007), "Free vibration of laminated and sandwich plates using enhanced plate theories", *J. Sound Vib.*, **308**(1-2), 268–286. https://doi.org/10.1016/j.jsv.2007.07.040.

Kumari, P. and Behera, S. (2017a), "Three-dimensional free vibration analysis of levy-type laminated plates using multi-term extended Kantorovich method", *Compos. Part B Eng.*, **116**, 224–238. https://doi.org/10.1016/j.compositesb.2017.01.057.

Kumari, P. and Behera, S. (2017b), "Three-dimensional free vibration analysis of levy-type laminated plates using multi-term extended Kantorovich method", *Compos. Part B Eng.*, **116**, 224–238. https://doi.org/10.1016/j.compositesb.2017.01.057.

Kumari, P., Kapuria, S. and Rajapakse, R. (2014), "Three-dimensional extended Kantorovich solution for Levy-type rectangular laminated plates with edge effects", *Compos. Struct.*, **107**, 167–176. https://doi.org/10.1016/j.compstruct.2013.07.053.

Kumari, P., Nath, J., Dumir, P. and Kapuria, S. (2007), "2D exact solutions for flat hybrid piezoelectric and magnetoelastic angle-ply panels under harmonic load", *Smart Mater. Struct.*, **16**(5), 1651. https://doi.org/10.1088/0964-1726/16/5/018.

Kumari, P., Singh, A., Rajapakse, R. and Kapuria, S. (2017), "Three-dimensional static analysis of Levy-type functionally graded plate with in-plane stiffness variation", *Compos. Struct.*, **168**, 780–791. https://doi.org/10.1016/j.compstruct.2017.02.078.

Messina, A. (2001), "Two generalized higher order theories in free vibration studies of multilayered plates", *J. Sound Vib.*, **242**(1), 125–150. https://doi.org/10.1006/jsvi.2000.3364.

Messina, A. and Soldatos, K.P. (2002), "A general vibration model of angle-ply laminated plates that accounts for the continuity of interlaminar stresses", *J. Solids Struct.*, **39**(3), 617–635. https://doi.org/10.1016/S0020-7683(01)00169-X.

Pan, E. and Heyliger, P.R. (2003), "Exact solutions for magneto-electro-elastic laminates in cylindrical bending", *J. Solids Struct.*, **40**(24), 6859–6876. https://doi.org/10.1016/j.ijsolstr.2003.08.003.

Qing, G., Qiu, J. and Liu, Y. (2006), "A semi-analytical solution for static and dynamic analysis of plates with piezoelectric patches", *J. Solids Struct.*, **43**(6), 1388-1403. https://doi.org/10.1016/j.ijsolstr.2005.03.048.

Saravanos, D.A. and Heyliger, P.R. (1999), "Mechanics and computational models for laminated piezoelectric beams, plates, and shells", *Appl. Mech. Rev.*, **52**(10), 305–320. https://doi.org/10.1115/1.3098918.

Sayyad, A.S. and Ghugal, Y.M. (2015), "On the free vibration analysis of laminated composite and sandwich plates: A review of recent literature with some numerical results", *Compos. Struct.*, **129**, 177–201. https://doi.org/10.1016/j.compstruct.2015.04.007.

Sheng, H., Wang, H. and Ye, J. (2007), "State space solution for thick laminated piezoelectric plates with clamped and electric open-circuited boundary conditions", *J. Mech. Sci.*, **49**(7), 806–818. https://doi.org/10.1016/j.ijmecsci.2006.11.012.

Shu, X. (2005a), "Free vibration of laminated piezoelectric composite plates based on an accurate theory", *Compos. Struct.*, **67**(4), 375–382. https://doi.org/10.1016/j.compstruct.2004.01.022.

Shu, X. (2005b), "Modelling of cross-ply piezoelectric composite laminates in cylindrical bending with interfacial shear slip", *J. Mech. Sci.*, **47**(11), 1673–1692. https://doi.org/10.1016/j.ijmecsci.2005.07.003.

Singh, A., Kumari, P. and Hazarika, R. (2018), "Analytical Solution for Bending Analysis of Axially Functionally Graded Angle-Ply Flat Panels", *Math. Problems Eng.*, **2018**. https://doi.org/10.1155/2018/2597484.

Singhatanadgid, P. and Singhanart, T. (2017), "The Kantorovich method applied to bending, buckling, vibration, and 3D stress analyses of plates: A literature review", *Mech. Adv. Mater. Struct.*, pages 1–19. https://doi.org/10.1080/15376494.2017.1365984.

Singhatanadgid, P. and Singhanart, T. (2019), "The Kantorovich method applied to bending, buckling, vibration, and 3D stress analyses of plates: A literature review", *Mech. Adv. Mater. Struct.*, **26**(2), 170–188. https://doi.org/10.1080/15376494.2017.1365984.

Udayakumar, B. and Gopal, K.N. (2017), "A modified state space differential quadrature method for free vibration analysis of soft-core sandwich panels", *J. Sandwich Struct. Mater.*, https://doi.org/10.1177/1099636217727801.

Vel, S.S., Mewer, R. and Batra, R. (2004), "Analytical solution for the cylindrical bending vibration of

piezoelectric composite plates", *J. Solids Struct.*, **41**(5-6), 1625-1643. https://doi.org/10.1016/j.ijsolstr.2003.10.012.

Wu, C.P., Chiu, K.H. and Wang, Y.M. (2008), "A review on the three-dimensional analytical approaches of multilayered and functionally graded piezoelectric plates and shells", *Comput. Mater. Continua*, **8**(2), 93–132.

Wu, C.P. and Liu, Y.C. (2016), "A review of semi-analytical numerical methods for laminated composite and multilayered functionally graded elastic/piezoelectric plates and shells", *Compos. Struct.*, **147**, 1–15. https://doi.org/10.1016/j.compstruct.2016.03.031.

Xu, K., Noor, A.K. and Tang, Y.Y. (1997), "Three-dimensional solutions for free vibrations of initially-stressed thermoelectroelastic multilayered plates", *Comput. Methods Appl. Mech. Eng.*, **141**(1-2), 125–139. https://doi.org/10.1016/S0045-7825(96)01065-1.

Yan, W., Lv, T., Lei, T. and Zhi, J. (2019), "Exact analysis of imperfect angle-ply laminated panels with surface-bonded piezoelectric layers", *Arch. Appl. Mech.*, 1–12. https://doi.org/10.1007/s00419-018-01502-z.

Yang, J., Batra, R. and Liang, X. (1994), "The cylindrical bending vibration of a laminated elastic plate due to piezoelectric actuators", *Smart Mater. Struct.*, **3**(4), 485. https://doi.org/10.1088/0964-1726/3/4/011.

Yang, J., Batra, R.C. and Liang, X. (1995), "Vibration of a simply supported rectangular elastic plate due to piezoelectric actuators", *Smart Structures and Materials 1995: Mathematics and Control in Smart Structures,* Volume 2442, International Society for Optics and Photonics, Bellingham, WA, USA. 168-181.

Zhang, Z., Feng, C. and Liew, K. (2006), "Three-dimensional vibration analysis of multilayered piezoelectric composite plates", *J. Eng. Sci.*, **44**(7), 397–408. https://doi.org/10.1016/j.ijengsci.2006.02.002.

Zhou, Y., Chen, W. and Lü, C. (2010), "Semi-analytical solution for orthotropic piezoelectric laminates in cylindrical bending with interfacial imperfections", *Compos. Struct.*, **92**(4), 1009–1018. https://doi.org/10.1016/j.compstruct.2009.09.048.

Zhou, Y., Chen, W., Lü, C. and Wang, J. (2009), "Free vibration of cross-ply piezoelectric laminates in cylindrical bending with arbitrary edges", *Compos. Struct.*, **87**(1), 93–100. https://doi.org/10.1016/j.compstruct.2008.01.002.

CC

Appendix A

The nonzero elements of $\mathbf{M}$, $\bar{\mathbf{A}}^{\mathbf{m}}, \hat{\mathbf{A}}^{\mathbf{m}}, \mathbf{K}^{\mathbf{m}}, \tilde{\mathbf{A}}^{\mathbf{m}}$, matrices of Eqs. (21) and (22) are given below

$$
\begin{aligned}
&M_{i_1 j_1} = M_{j_6 i_6} = \langle f_8^i f_1^j \rangle_a, \quad M_{i_2 j_2} = M_{j_5 i_5} = \langle f_7^i f_2^j \rangle_a, \quad M_{i_3 j_3} = M_{j_4 i_4} = \langle f_5^i f_3^j \rangle_a \\
&M_{i_7 j_7} = M_{j_8 i_8} = \langle f_{11}^i f_9^j \rangle_a, \quad \bar{A}_{i_1 j_3} = \frac{-t}{a} \langle f_8^i f_{3,\xi}^j \rangle_a, \quad \bar{A}_{i_1 j_5} = tp_{45} \langle f_8^i f_7^j \rangle_a \\
&\bar{A}_{i_1 j_6} = tp_{55} \langle f_8^i f_8^j \rangle_a, \quad \hat{A}_{i_1 j_3} = tp_{57} \langle f_8^i f_{10}^j \rangle_a, \quad \bar{A}_{i_2 j_5} = tp_{44} \langle f_7^i f_7^j \rangle_a \\
&\bar{A}_{i_2 j_6} = tp_{45} \langle f_7^i f_8^j \rangle_a, \quad \hat{A}_{i_2 j_3} = tp_{47} \langle f_7^i f_{10}^j \rangle_a, \quad \bar{A}_{i_3 j_4} = tp_{33} \langle f_5^i f_5^j \rangle_a \\
&\bar{A}_{i_3 j_8} = tp_{38} \langle f_5^i f_{11}^j \rangle_a, \quad \hat{A}_{i_3 j_1} = tp_{31} \langle f_5^i f_4^j \rangle_a, \quad \hat{A}_{i_3 j_2} = tp_{36} \langle f_5^i f_6^j \rangle_a \\
&\bar{A}_{i_4 j_6} = \frac{-t}{a} \langle f_3^i f_{8,\xi}^j \rangle_a, \quad \hat{A}_{i_5 j_2} = \frac{-t}{a} \langle f_2^i f_{6,\xi}^j \rangle_a, \quad \hat{A}_{i_6 j_1} = \frac{-t}{a} \langle f_1^i f_{4,\xi}^j \rangle_a \\
&\bar{A}_{i_7 j_4} = tp_{83} \langle f_{11}^i f_5^j \rangle_a, \quad \bar{A}_{i_7 j_8} = tp_{88} \langle f_{11}^i f_{11}^j \rangle_a, \quad \hat{A}_{i_7 j_1} = tp_{81} \langle f_{11}^i f_4^j \rangle_a \\
&\hat{A}_{i_7 j_2} = tp_{86} \langle f_{11}^i f_6^j \rangle_a, \quad \hat{A}_{i_8 j_3} = \frac{-t}{a} \langle f_9^i f_{10,\xi}^j \rangle_a, \quad K_{i_1 j_1} = p_{11} \langle f_4^i f_4^j \rangle_a \\
&K_{i_1 j_2} = p_{16} \langle f_4^i f_6^j \rangle_a, \quad K_{j_2 i_1} = K_{i_1 j_2}, \quad K_{i_2 j_2} = p_{66} \langle f_6^i f_6^j \rangle_a \\
&K_{i_3 j_3} = p_{77} \langle f_{10}^i f_{10}^j \rangle_a, \quad \tilde{A}_{i_1 j_1} = \frac{1}{a} \langle f_4^i f_{1,\xi}^j \rangle_a, \quad \tilde{A}_{i_1 j_4} = -p_{13} \langle f_4^i f_5^j \rangle_a \\
&\tilde{A}_{i_1 j_8} = -p_{18} \langle f_4^i f_{11}^j \rangle_a, \quad \tilde{A}_{i_2 j_2} = \frac{1}{a} \langle f_6^i f_{2,\xi}^j \rangle_a, \quad \tilde{A}_{i_2 j_4} = -p_{63} \langle f_6^i f_5^j \rangle_a \\
&\tilde{A}_{i_2 j_8} = -p_{68} \langle f_6^i f_{11}^j \rangle_a, \quad \tilde{A}_{i_3 j_5} = p_{74} \langle f_{10}^i f_7^j \rangle_a, \quad \tilde{A}_{i_3 j_6} = p_{75} \langle f_{10}^i f_8^j \rangle_a \\
&\tilde{A}_{i_3 j_7} = \frac{-1}{a} \langle f_{10}^i f_{9,\xi}^j \rangle_a, \quad \bar{A}_{i_4 j_3} = -\rho\omega^2 t \langle f_3^i f_3^j \rangle_a, \quad \bar{A}_{i_5 j_2} = -\rho\omega^2 t \langle f_2^i f_2^j \rangle_a \\
&\bar{A}_{i_6 j_1} = -\rho\omega^2 t \langle f_1^i f_1^j \rangle_a
\end{aligned}
\tag{A.1}
$$

where the notation $\langle ... \rangle_a = a \int_0^1 (...) d\xi$ represents integration over the span length a. Since the functions f_l^i are known analytical functions, elements of the matrices defined in Eqs. (A.1) and have been evaluated in closed form.

Appendix B

Using the notation $\langle ... \rangle_h = \sum_{k=1}^{L} t^{(k)} \int_0^1 (...)^{(k)} d\zeta$ for integration across the thickness, the nonzero elements of $\mathbf{N}$, $\bar{\mathbf{B}}^{\mathbf{f}}, \hat{\mathbf{B}}^{\mathbf{f}}, \mathbf{L}^{\mathbf{f}}$ and $\tilde{\mathbf{B}}^{\mathbf{f}}$ Eqs.(29) and (30) are given below

$$
\begin{aligned}
&N_{i_1 j_1} = N_{j_4 i_4} = \langle g_4^i g_1^j \rangle_h, \quad N_{i_2 j_2} = N_{j_5 i_5} = \langle g_6^i g_2^j \rangle_h \\
&N_{i_3 j_3} = N_{j_6 i_6} = \langle g_8^i g_3^j \rangle_h, \quad N_{i_7 j_7} = N_{j_8 i_8} = \langle g_{10}^i g_9^j \rangle_h
\end{aligned}
\tag{B.1}
$$

$$B_{i_1 j_4} = \langle \bar{p}_{11} g_4^i g_4^j \rangle_h, \quad \bar{B}_{i_1 j_5} = \langle \bar{p}_{16} g_4^i g_6^j \rangle_h, \quad \hat{B}_{i_1 j_1} = \langle \bar{p}_{13} g_4^i g_5^j \rangle_h, \quad \bar{B}_{i_1 j_7} = -\langle \bar{p}_{18} g_4^i \frac{g_{9,\zeta}^j}{t} \rangle_h$$

$$\bar{B}_{i_2 j_4} = \langle \bar{p}_{61} g_6^i g_4^j \rangle_h, \quad \bar{B}_{i_2 j_5} = \langle \bar{p}_{66} g_6^i g_6^j \rangle_h, \quad \hat{B}_{i_2 j_1} = \langle \bar{p}_{63} g_6^i g_5^j \rangle_h, \quad \bar{B}_{i_2 j_7} = -\langle \bar{p}_{68} g_6^i \frac{g_{9,\zeta}^j}{t} \rangle_h$$

$$\bar{B}_{i_3 j_1} = -\langle g_8^i \frac{g_{1,\zeta}^j}{t} \rangle_h, \quad \bar{B}_{i_3 j_6} = \langle p_{55} g_8^i g_8^j \rangle_h, \quad \hat{B}_{i_3 j_2} = \langle p_{45} g_8^i g_7^j \rangle_h, \quad \bar{B}_{i_3 j_8} = \langle p_{57} g_8^i g_{10}^j \rangle_h$$

$$\bar{B}_{i_4 j_6} = \langle \frac{g_{1,\zeta}^i}{t} g_8^j \rangle_h, \quad \hat{B}_{i_5 j_2} = \langle \frac{g_{2,\zeta}^i}{t} g_7^j \rangle_h, \quad \hat{B}_{i_6 j_1} = \langle g_3^i \frac{g_{5,\zeta}^j}{t} \rangle_h, \quad \bar{B}_{i_7 j_6} = \langle p_{75} g_{10}^i g_8^j \rangle_h$$

$$\bar{B}_{i_7 j_8} = -\langle p_{77} g_{10}^i g_{10}^j \rangle_h, \ \hat{B}_{i_7 j_2} = \langle p_{74} g_{10}^i g_7^j \rangle_h, \ \hat{B}_{i_8 j_3} = -\langle g_9^i \frac{g_{11,\zeta}^j}{t} \rangle_h, \ L_{i_1 j_1} = \langle \bar{p}_{33} g_5^i g_5^j \rangle_h \tag{B.2}$$

$$\tilde{B}_{i_1 j_7} = \langle \bar{p}_{38} g_5^i \frac{g_{9,\zeta}^j}{t} \rangle_h, \ L_{i_2 j_2} = \langle p_{44} g_7^i g_7^j \rangle_h, \quad L_{i_3 j_1} = \langle \bar{p}_{83} g_{11}^i g_5^j \rangle_h, \ L_{i_3 j_3} = \langle \bar{p}_{88} g_{11}^i g_{11}^j \rangle_h$$

$$\tilde{B}_{i_1 j_3} = \langle g_5^i \frac{g_{3,\zeta}^j}{t} \rangle_h, \quad \tilde{B}_{i_1 j_4} = -\langle \bar{p}_{31} g_5^i g_4^j \rangle_h, \ \tilde{B}_{i_1 j_5} = -\langle \bar{p}_{36} g_5^i g_6^j \rangle_h, \ \tilde{B}_{i_2 j_2} = \langle g_7^i \frac{g_{2,\zeta}^j}{t} \rangle_h$$

$$\tilde{B}_{i_2 j_6} = -\langle p_{45} g_7^i g_8^j \rangle_h, \ \tilde{B}_{i_2 j_8} = -\langle p_{47} g_7^i g_{10}^j \rangle_h, \ \tilde{B}_{i_3 j_4} = -\langle \bar{p}_{81} g_{11}^i g_4^j \rangle_h, \ \tilde{B}_{i_3 j_5} = -\langle \bar{p}_{86} g_{11}^i g_6^j \rangle_h$$

$$\tilde{B}_{i_3 j_7} = \langle g_{11}^i \frac{g_{9,\zeta}^j}{t} \rangle_h, \bar{B}_{i_4 j_1} = -a\rho\omega^2 \langle g_1^i g_1^j \rangle_h, \ \bar{B}_{i_5 j_2} = -a\rho\omega^2 \langle g_2^i g_2^j \rangle_h, \ \bar{B}_{i_6 j_3} = -a\rho\omega^2 \langle g_3^i g_3^j \rangle_h$$

Since $g_l^i(\zeta)$ are known in close form, all integrations in Eqs. (B.1) and (B.2) are evaluated exactly in closed form.